CO_2-ASSISTED GRAVITY DRAINAGE EOR: NUMERICAL SIMULATION AND SCALING MODELS STUDY

A thesis

Submitted in the fulfilment of the
requirements for the degree of

Doctor of Philosophy
in
Petroleum Engineering

By

Prashant Jadhawar
B. Eng. in Petroleum Eng., University of Pune, India
M. Eng. in Petroleum Eng., University of Pune, India
M. Phil. in Petroleum Eng., Heriot-Watt University, UK

Australian School of Petroleum
Faculty of Engineering, Chemical and Mathematical Sciences (ECMS)
The University of Adelaide, Australia

September 2010

6 OIL RECOVERY OPTIMIZATION

Review of the reservoir simulation and field studies indicate that the gravity drainage process for enhancing the oil recovery has not yet been investigated in secondary mode CO_2 injection in immiscible and miscible process. Moreover, there is no reported field or case study of compositional reservoir simulations on 50 ^{o}API gravity oil in immiscible and miscible gravity drainage oil recovery method. This lacking research opportunity is exploited in this Chapter.

Investigations are carried out to study the effects of grid size through grid-refinement studies, miscibility development, heterogeneity, molecular diffusion, and the mode of gas injection on the CO_2-assisted gravity drainage EOR method. Concurrent operational mechanisms that are contributing the enhanced oil recovery in the respective process are also discussed with the supporting figures and illustrations. The results presented herein are obtained thereby conducting the reservoir simulations over the pseudomiscible and Equation-Of-State based compositional models using CMG's IMEX and GEM simulators.

Critical and stable gas injection rates are calculated using the multiphase process parameters to satisfy the stable gas floodfront criteria by Dumore (1964a). These are presented in **Appendix-B.** In all of the reservoir simulation runs, the CO_2 injection rates are kept lower than the critical and stable rates to avoid the injection gas fingering through the oil-zone and premature breakthrough at the horizontal production wells placed at the bottom of the oil zone.

6.1 Mechanisms Identification and General Process Selection Map Development: CO_2-Assisted Gravity Drainage EOR Process

Effects of the miscibility development on CO_2-assisted gravity drainage enhanced oil recovery are investigated through compositional simulations on the 50 ^{o}API gravity oil from an Australian reservoir.

Seven combinations (successively higher) of CO_2 injection and oil production rates (see **Table 6-1**) are used to obtain the oil recovery performance in immiscible and miscible process while maintaining the voidage balance conditions during gravity drainage

recovery. First four rate constraints are the same that were investigated in the immiscible and miscible well pattern studies (section 5.4 of Chapter-5). At higher pressure CO_2 injection in case of miscible process, higher rates were required for the same oil production rates in immiscible process. Regular well pattern of the vertical CO_2 injection and horizontal oil production wells, that yield the optimized oil recovery (based on the findings in Chapter 5), is used in this study.

Reservoir simulations are conducted in both the immiscible and miscible CO_2-assisted gravity drainage EOR process for 132 years of secondary mode CO_2 injection. Results of the sensitivity analysis in seven well-constraint combinations, to achieve the optimized recovery and study the associated operational mechanisms, are then compared.

Table 6-1: Rate constraints of the wells

Case	Rate constraints/well		
	i_{CO2}, MMSCFD		q_o, BPD
	Immisicble	Miscible	
I	1.50E+06	2.09E+06	4000
II	3.32E+06	4.70E+06	9000
III	5.62E+06	7.80E+06	15000
IV	1.00E+07	1.40E+07	20000
V	2.00E+07	2.74E+07	52500
VI	3.00E+07	4.10E+07	80000
VII	4.00E+07	5.60E+07	108000

Incremental oil recovery performance in all the immiscible and miscible rate-constraints for the respective pore volumes of CO_2 injected is presented in **Figure 6-1** and **Figure 6-2**. This recovery is the volume of oil recovered out of the volume that was present in oil zone at the start of secondary mode CO_2 injection (the incremental) for the respective incremental pore volumes injected.

$$\text{Incremental EOR} = \frac{\text{Incremental Oil Recovered in } CO_2\text{-Assisted Gravity Drainage process}}{\text{Oil-In-Place at the start of } CO_2 \text{ injection}}$$

Results in **Figure 6-1** show that immiscible process yields higher recovery than the miscible flood in first two low rate-constraint combinations. In Case-III and Case-IV, miscible recovery is marginally higher than the immiscible recovery for 0.25 and 0.45 pore volumes of CO_2 injected (PV_{CO2inj}).

For higher rate-combinations of Case-V, incremental oil recovery in miscible process (red curve) found to be distinctively higher than the immiscible process (green curve) at 0.89 PV_{CO2inj}. CO_2 floodfront arrived 30 years earlier than Case-IV (see **Figure 6-3**). This provided more time for the continuous gas-phase behind CO_2 floodfront to interact with the trapped oil in the pores. Miscible incremental oil recovery (red curve) further increased in Case-VI in comparison with the incremental oil recovery in immiscible process (green curve) at 1.34 PV_{CO2inj}. Although gas floodfront arrived merely 7 years earlier than the Case-V, the higher recovery indicates that the mechanisms in miscible flood are more effective in recovering the trapped oil.

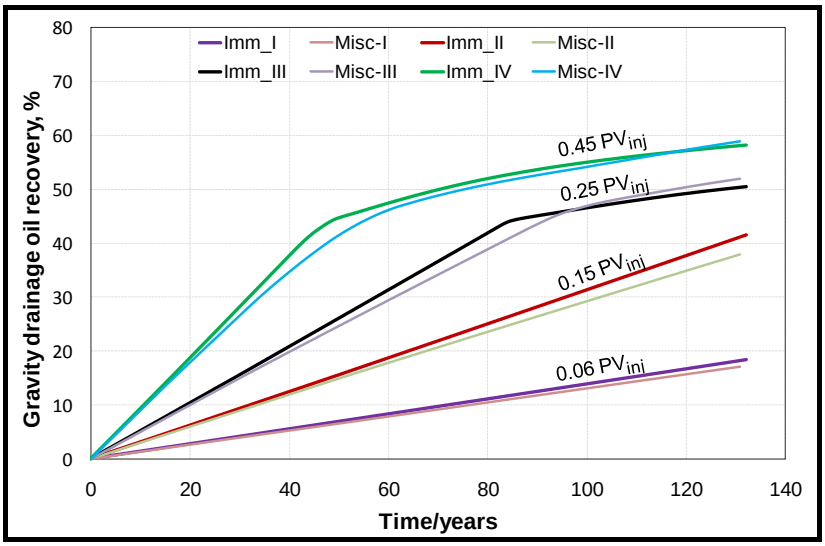

Figure 6-1: Comparison of the incremental immiscible and miscible CO_2-assisted gravity drainage oil recovery in rate-constraints from Case-I to Case-IV

At higher CO_2 injection rate (in Case-VII), incremental recovery in miscible CO_2-assisted gravity drainage EOR process was highest than the immiscible flood (see **Figure 6-2**) amongst all the earlier well rate-constraints from Case-I to Case-VI. Highest incremental recovery of 79% in miscible flood was obtained. It is 10% higher than the immiscible flood (69%). GOC reached 4 years earlier than Case-VI, thus providing higher time for interaction of trapped oil with the continuous gas phase behind the gas-oil contact (CO_2 floodfront).

Careful inspection of the above results (see **Figure 6-1** and **Figure 6-2**) indicates that there is a definitive trend in the incremental oil recoveries. Immiscible recovery dominates the miscible recovery before the leading edge of CO_2 floodfront arrive in the

drainage area of horizontal wells. However, oil recovery in miscible process overlaps the immiscible process after CO_2 floodfront arrival. This suggests that the mechanisms that contribute higher recovery in the miscible flood are more effective in draining trapped oil from the pores behind the CO_2 floodfront than the contributing active mechanisms reminiscent in the immiscible flood. This further implies that the mechanisms that are operational in immiscible process, especially after CO_2 floodfront arrival are exceedingly slower than those prevalent in miscible process. What are those mechanisms and how they contribute the incremental oil recovery, is discussed in the later section.

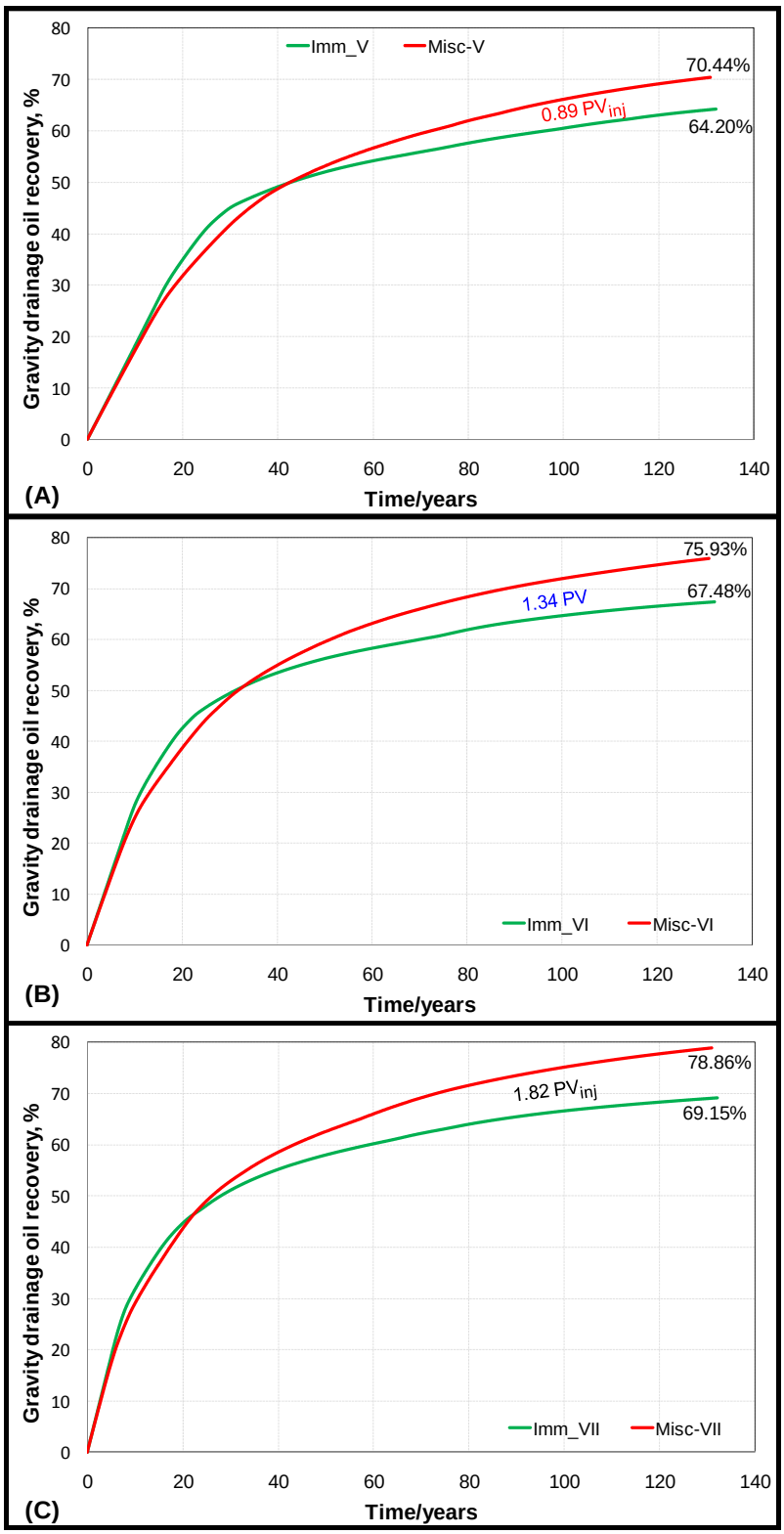

Figure 6-2: Comparison - Incremental CO_2-assisted gravity drainage oil recoveries in both the immiscible and miscible process from Case-V to Case-VII

Profile of Gas-oil ratio (GOR) for the rate-constraints from Case-IV to Case-VII (see **Table 6-1**) is as shown on **Figure 6-3**. Thick curves represent the GOR for immiscible

process for the adjoining thin curves depicting GOR for the miscible process. GOR for both the immiscible and miscible floods remains at solution GOR values resulting in the single phase flow until the CO_2 floodfront arrival. It kept rising later. GORs for miscible process appear to be lower than the immiscible process in each of the successive higher well rate-constraint combinations. Maximum GOR of 96000 was observed immiscible process than 85875 in miscible process for Case-VII. As the reservoir oil is very light oil of 50 ^{o}API gravity, the gas condensate production may have caused the GOR in immiscible flood to rise to levels than those in the miscible process. Conversely, the high pressure miscible CO_2 injection could have compressed the condensate gas, which is then being produced after gas breakthrough at lower GOR rates.

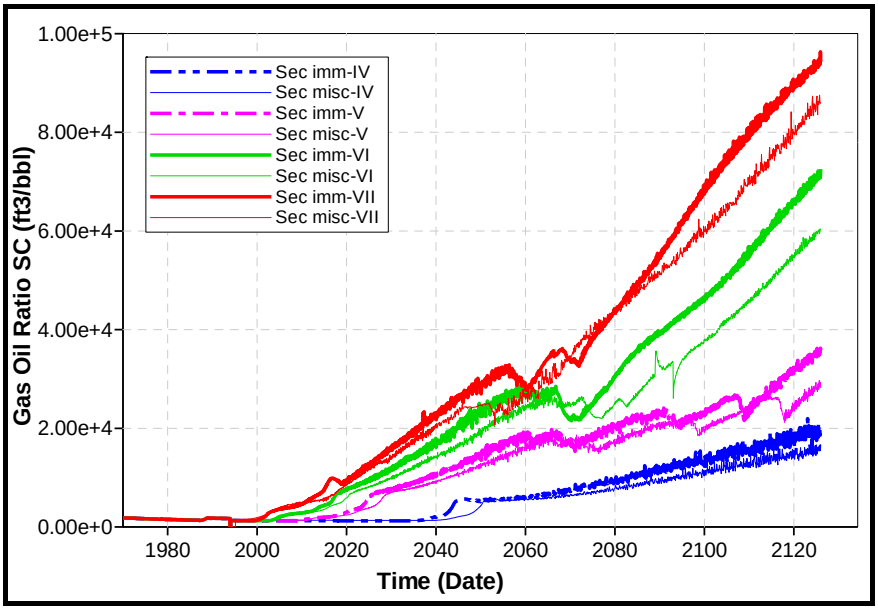

Figure 6-3: Gas-oil ratio (GOR) comparison from Case-IV through Case-VII during operation of the immiscible and miscible CO_2-assisted gravity drainage EOR process

Water production profile for all the four (Case-IV to Case-VII) immiscible and miscible floods in top-down gravity drainage process indicates that water breakthrough from the underlying aquifer is zero or exceeding low (see **Figure 6-4**). Reason is that the horizontal wells are perforated parallel to the horizontal bedding plane containing water zone in non-dipping horizontal type reservoir. This, in addition to the vertical-downward CO_2 injection, prevents water coning further aiding in the downward-gravity drainage of the oil from the upper layers. Therefore two-phase flow of gas and oil is observed in

secondary immiscible and miscible CO_2-assisted gravity drainage EOR process, especially after the gas floodfront arrival in horizontal wells.

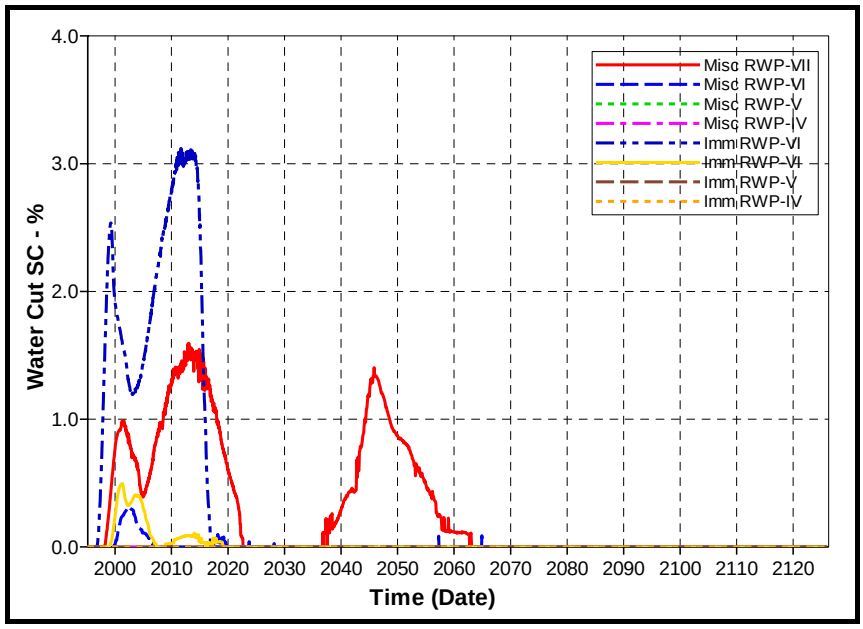

Figure 6-4: Water breakthrough in all the seven immiscible and miscible CO_2-assisted gravity drainage floods.

6.1.1 Overall Mechanisms: Immiscible and Miscible Process

In both the immiscible and miscible CO_2-assisted gravity drainage EOR processes, the average reservoir pressure is a parameter that itself demonstrate the involved oil recovery contributing mechanism. To understand this, oil rate (bpd), gas-oil ratio (GOR) and the average reservoir pressure in both the immiscible and miscible process of Case-V are plotted as shown in **Figure 6-5.**

Average reservoir pressure at the start of immiscible CO_2 flood was 2633 psia in March 1995 while at the end (April 2126), it was 2598 psia (**Figure 6-5A)**. It dropped by just 35 psia at an average rate of 0.26 psia per year in 132 years of immiscible CO_2 injection and simultaneous production. Oil production starts immediately after CO_2 injection (**Figure 6-5A)**. Water phase being immobile, the single phase flow of oil (associated gas production is the solution gas) is observed in the secondary CO_2 flood. Higher density difference between oil and gas during immiscible secondary flood promotes the oil drainage under gravity behind the CO_2 floodfront. This drained oil joins the oil bank formed ahead of the CO_2 floodfront further contributing the oil-displacement taking place ahead of the CO_2 floodfront. Oil bank constitutes the majority of oil in the oil-bearing zone

that is produced through Buckley-Leverett type of displacement (1942). Once it is immiscibly displaced through Darcy flow representative of the B-L theory, leading edge of the CO_2-floodfront reaches the drainage area of the horizontal production wells resulting in the gas breakthrough as shown in **Figure 6-5A**. The decline of oil rate and the corresponding increase in GOR represents the arrival of the leading edge of the CO_2 floodfront in the drainage area of the horizontal oil production wells. In spite of this, the reservoir pressure did not decline considerably in this phase of the oil production. After gas breakthrough, the oil production continued at a lower but gradually declining rate. Even in this later phase, the reservoir pressure did not show drastic reduction. This negligible pressure drop at reservoir scale suggests that the pressure in the gas-cap behind CO_2 floodfront could be constant thereby satisfying Cardwell Parson's criteria (1949b) of free gravity drainage. Similar behaviour was observed before and after gas breakthrough in well pattern studies of immiscible flood as discussed in section 5.4.1 of chapter-5 (**Figure 5-13A**, **Figure 5-13B** and **Figure 5-16B**).

In high pressure CO_2 miscible flood (see **Figure 6-5B)**, reservoir pressure declined by 60 psia until the CO_2 floodfront arrival in drainage area of all of the horizontal production wells in the year 2022 (2.22 psi/year). This shows that miscible CO_2 injection forms a bulk-oil zone followed by the oil-solvent mixed miscible bank behind CO_2 floodfront. Single phase Darcy displacement of bulk-oil, characterized by Buckley-Leverett theory (see section 2.3.3) (1942), is observed before CO_2 breakthrough followed by the low-rate oil production through gravity drainage. CO_2 floodfront arrival is marked by rise in GOR for the corresponding drop in oil production. Furthermore, **Figure 6-5B** demonstrates that the reservoir pressure drop is zero for 104 years after the gas floodfront arrival. This constant reservoir pressure behaviour, in turn, is asymptotic of the constant reservoir pressure in the gas-cap, thus strictly satisfying the Cardwell Parson's criteria (1949b) of free-fall gravity drainage oil recovery. There could be additional mechanisms contributing this gravity drainage enhanced oil recovery which are discussed in the following sections.

In order to compare the reservoir pressure profiles of other Case-IV, Case-VI and Case-VII with the Case-V, **Figure 6-6** was plotted for both the immiscible and miscible CO_2-assisted gravity drainage EOR process.

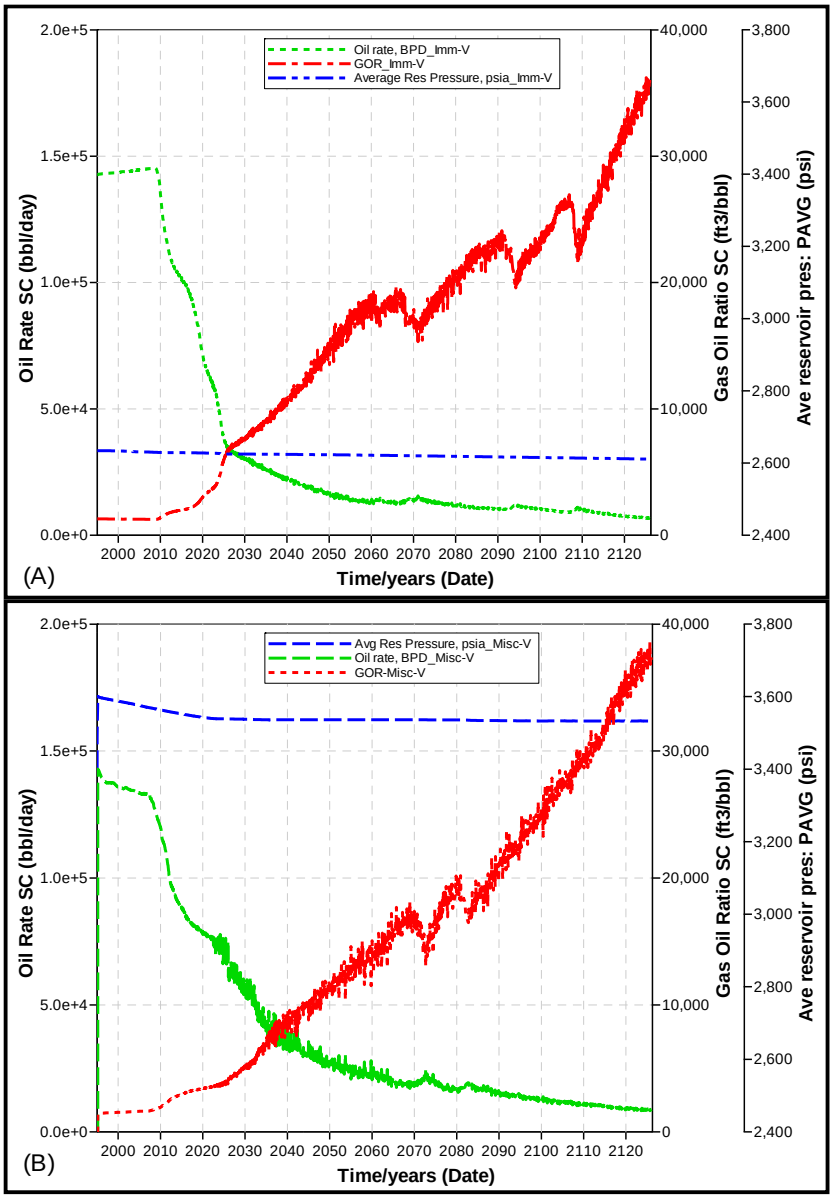

Figure 6-5: Profile of the oil rate, GOR and average reservoir pressure in (A) immiscible and (B) miscible process (Case-V)

In immiscible process, the average reservoir pressure at the start of secondary CO_2 flood was 2633 psia (**Figure 6-6A)**. It drops by 22, 70 and 100 psi in Case-IV, Case-VI and Case-VII respectively in 132 years of production. This means that the respective average pressure drop during this period was more with the higher well rate-constraints, which are 0.17 psi, 0.54 psi and 0.77 psi per year respectively. This profile of the pressure drop before and after CO_2 floodfront arrival is similar to that observed in Case-V. Oil and the associated solution gas are produced through B-L piston type displacement (1942) before gas breakthrough, which is supported by gravity drainage of oil behind the CO_2 floodfront joining the bulk-oil zone. After gas breakthrough, the oil production rate

dropped considerably, but continued at a lower, but gradually declining rate. During this phase, very minimal pressure drop at reservoir scale further signifies the existence of constant pressure in the gas-cap behind CO_2 floodfront and the criterion of the free-fall gravity drainage by Cardwell and Parsons (1949b).

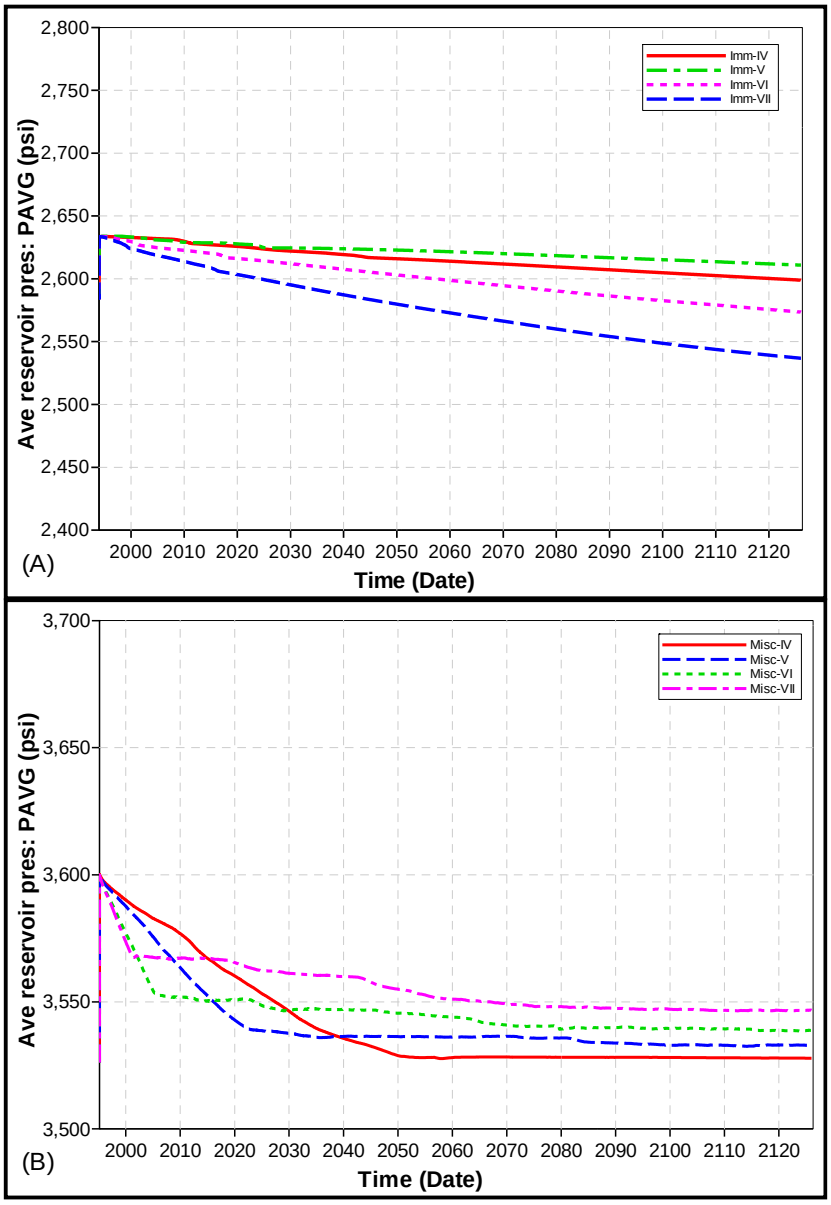

Figure 6-6: Average reservoir pressure comparison in Case-IV through Case-VII (A) immiscible and (B) miscible process

In CO_2 miscible flood, reservoir pressure for Case-IV combination resulted in its drop of 70 psia in 55 years (1.27 psi/year) until CO_2 floodfront arrival (**Figure 6-6B)**. It remains constant for the remaining flood of 56 years. This behaviour is very similar to

Case-V. This profile thus indicates the existence of B-L type displacement (1942) signifying the forced gravity drainage before CO_2 floodfront arrival and the free gravity drainage mechanism thereafter (1949b).

Average reservoir pressure dropped by 48 and 32 psi in 2006 (Case-VI) and 2001 (Case-VII) respectively when the CO_2 floodfront arrived the horizontal production wells. This pressure decline rate was 4.36 psi/year and 5.33 psi/year for Case-VI and Case-VII respectively. Such pressure decline represents the piston type displacement advocated by Buckley-Leverett theory (1942) signifying the forced gravity drainage oil recovery until CO_2 floodfront arrival and gas breakthrough. Thereafter the reservoir pressure either remains constant for few years (25 to 50 years) such as in Case-VI or decline very gradually about 16 psi in 125 years (Case-VII). This observation at reservoir scale is again asymptotic of the Cardwell Parson's fundamental criteria (1949b) signifying the free-fall gravity drainage oil recovery mechanism after gas breakthrough.

There could be additional mechanisms occurring concurrently contributing the gravity drainage oil recovery in both the immiscible and miscible CO_2-assisted gravity drainage EOR process. These are discussed in the following sections.

6.1.2 Contributing Mechanisms: Immiscible CO_2-Assisted Gravity Drainage EOR Process

In order to further analyse other mechanisms, a representative block (21, 20, 7) is chosen to demonstrate the oil saturation profile in combination with the reservoir pressure and GOR. **Figure 6-7** shows changes occurred in these associated properties over 132 years in immiscible CO_2 assisted gravity drainage EOR process (Case-V: **Figure 6-7A** and VII: **Figure 6-7B**).

In immiscible process, the oil saturation in block (21,20,7) stays constant at 0.82 for 16 and 7 years in case-V and VII respectively. The respective oil recovery was associated with the solution GOR yielding single phase flow. This indicated the B-L type displacement of bulk-oil production ahead of gas floodfront. Once it is produced, the leading edge of gas floodfront approaches the horizontal producing wells, yielding gas breakthrough. As shown in **Figure 6-7A** and **Figure 6-7B**, oil saturation then suddenly drops to 0.08 pointing out that majority of the reservoir oil is produced through B-L type displacement (Darcy flow) during this stage.

After gas breakthrough, oil saturation is constant for another 80 years (until 2090 in Case-V) suggesting that oil is continuously being drained from this block (21,20,7) before gradually declining to zero in 2126 (36 years later). At higher rate combination in Case-VII, same oil saturation took 55 years to drain oil from block (21,20,7), which is less than Case-V.

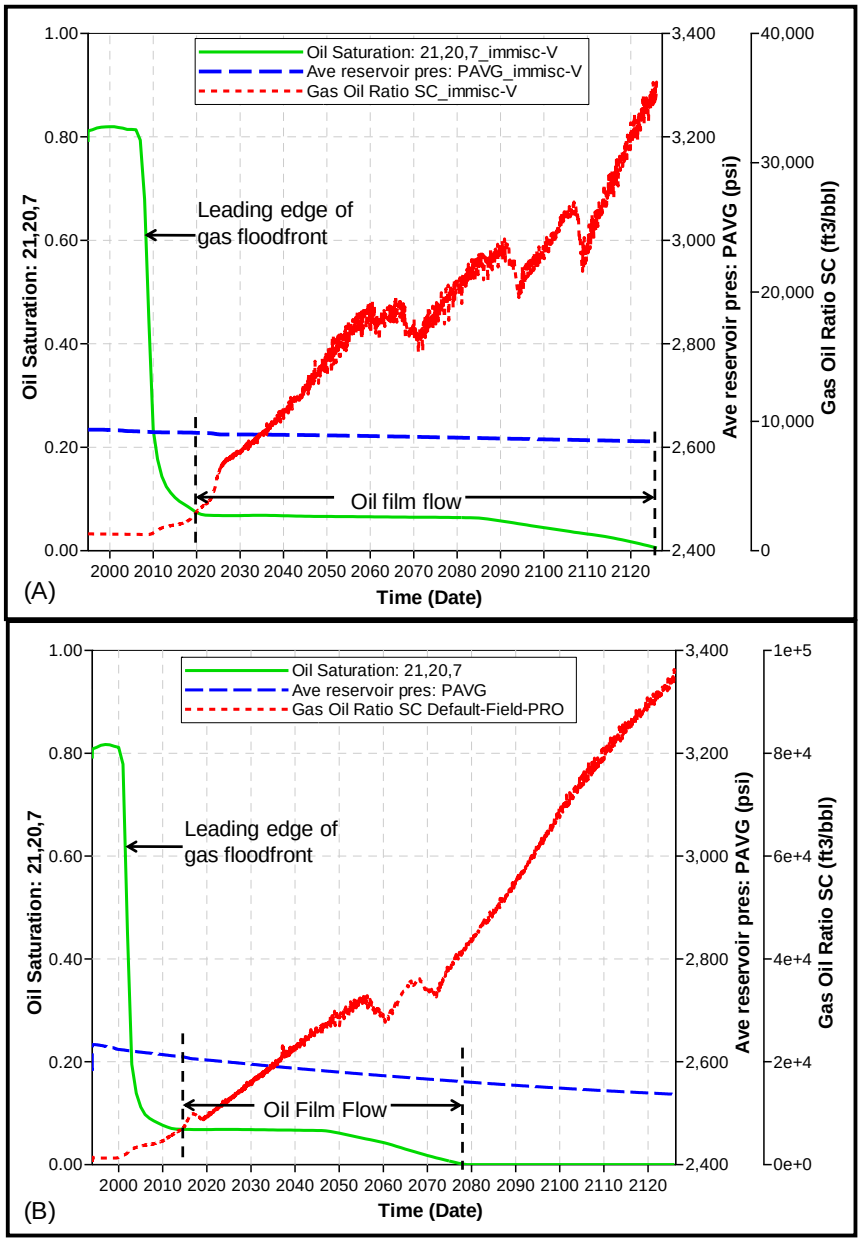

Figure 6-7: Existence of oil film flow demonstrated by the oil drainage behind the CO_2 floodfront in CO_2-assisted gravity drainage EOR process (A) Case-V and (B) Case-VII

Literature review suggests that there exist a mechanism called 'oil film flow' is responsible for this recovery. In the secondary immiscible CO_2 injection, the continuous

gas phase (instead of water phase in tertiary CO_2 injection) never forms contact with the immobile water phase. Instead, oil forms the layers of inter-connected film on immobile water phase and flows between the continuous gas phase and immobile water phase. It is thermodynamically stable thereby improving relative permeability to oil and providing high permeability pathways for oil drainage. Oil from the displaced oil zone behind the gas floodfront is drained under gravity downward towards the horizontal producers through these oil films.

Similar results are obtained in all the immiscible Case-I to Case-VII well-rate constraint combinations. There will be regions of reservoir where oil film gravity drainage occurring concurrently with other micro-mechanisms. Case-IV results have already been discussed, with regards to those other mechanisms, through gas saturation, oil viscosity and oil saturation properties of the block (45,24,6) in the section 5.4.1.2 of Chapter-5. These results of immiscible flood indicate that there exist the mechanisms of swelling and vaporization that occur along with the oil film flow. It is important to note here that the final incremental oil recoveries (%) obtained in immiscible Case-IV, V, VI and VII well rate constraints are 58.25, 64.20, 67.48 and 69.15 respectively.

6.1.3 Contributing Mechanisms: Miscible CO_2-Assisted Gravity Drainage EOR Process

Comparative results presented at beginning of this section (section 6.1) show that the incremental recovery in miscible flood is higher than those in immiscible process. The mechanisms that are responsible for this higher recovery are investigated in this section with the help of gas saturation, oil viscosity and the oil saturation properties. For this, the representative blocks (25,14,6), (25,14,7) and (25,14,8) of Case-VII well rate-constraint combination are chosen to track changes in these properties during the vertical-downward displacement of gas and oil phases.

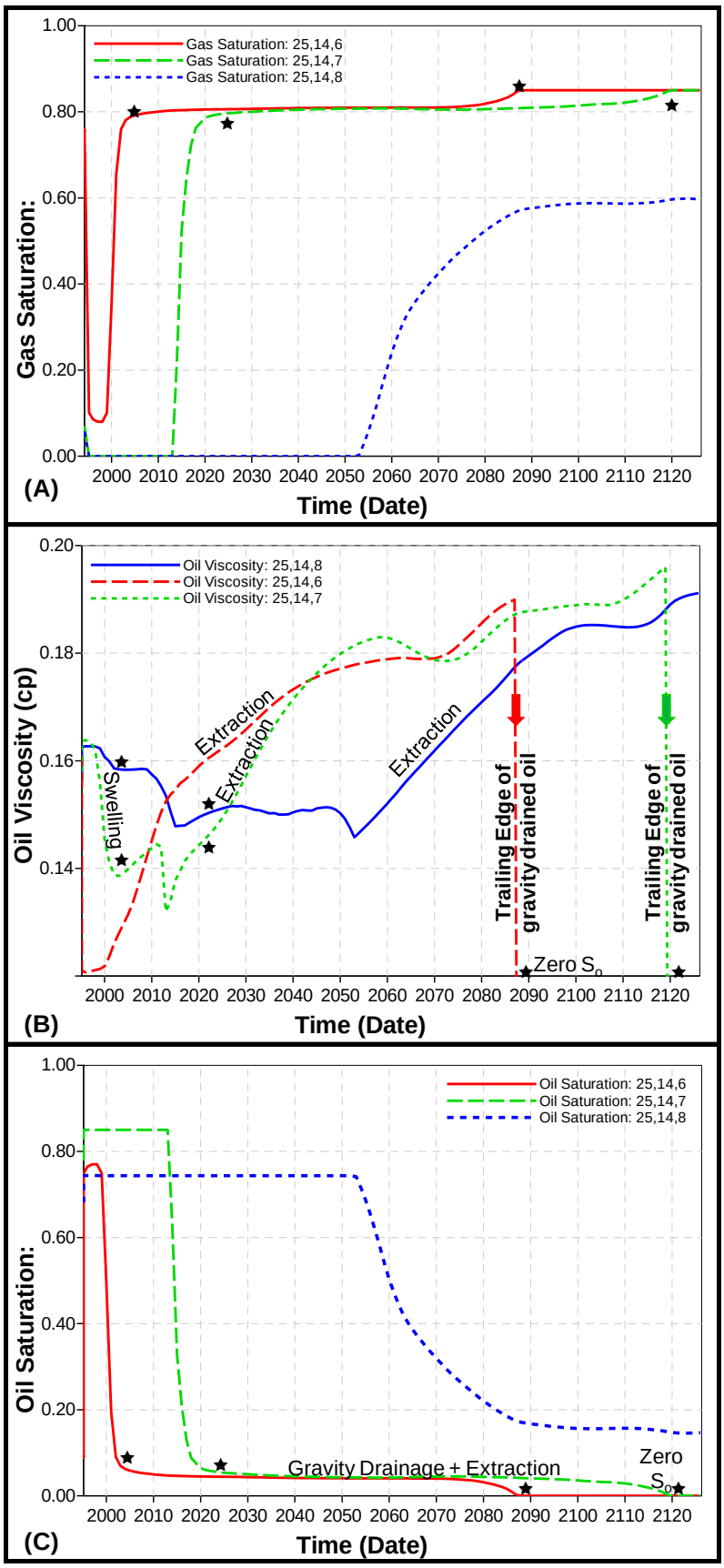

Figure 6-8: Mechanisms other than the CO_2-assisted gravity drainage in the blocks (25,14,6), (25,14,7) and (25,14,8) in the top-down miscible process

As shown in **Figure 6-8C**, oil saturation in block (25,14,6) gradually increased with the corresponding sharp drop of gas saturation (0.80 to 0.10) in 8 years from the start of miscible flood in year 1995. Once the gas front arrived in this upper block, which is in the immediate proximity of the gas-cap, gas saturation regained original value of 0.80 (see **Figure 6-8A**) and remain there for 65 years (until 2070). Respective oil saturation sharply declined to 0.10 value and continue to decline very gradually while yielding slow oil recovery (**Figure 6-8C**). In spite of constant profile of S_g over 65 years, the oil viscosity continues to rise. It means that the medium to heavy components are being extracted from the reservoir oil in this block, leading to oil-volume reduction and its viscosity increase. Oil viscosity reaches the zero values in the year 2087 (**Figure 6-8B**) indicating that the block (25,14,6) witnessed the complete oil recovery. This is shown by the trailing edge of the gravity drained oil for the corresponding zero oil saturation (**Figure 6-8C**) and the maximum gas saturation values (**Figure 6-8A**).

Sharp rise in the gas saturation and abrupt decline in oil saturation in the block (25,14,7) is observed in the year 2013. It is marked by the arrival of gas floodfront. Until this time reservoir oil experienced both the oil swelling and minor extraction represented by the respective oil viscosity drop and rise in **Figure 6-8B.** However after gas floodfront arrival, the oil viscosity witnessed only its rise, suggesting that the extraction mechanism play important role in recovering the reservoir oil that is left behind the CO_2 floodfront. During this period the oil saturation values remained steady at values about 0.04 (see **Figure 6-8C**). Once reservoir oil from upper block (25,14,6) is gravity drained downward in this block (25,14,7), oil saturation start to decline very gradually before its complete recovery in the year 2120 (32 years after gas floodfront arrival). Sudden vertical drop of the viscosity values represented the trailing edge of the gravity drained oil leaving this block (25,14,7).

The block (25,14,8) shown similar gas saturation, oil viscosity and oil saturation profile. Gas floodfront arrival is marked by the oil saturation reduction and gas saturation rise. Oil viscosity experienced its reduction coming from its swelling before CO_2 floodfront arrival and its consistent rise later. This result again point out that the reservoir oil behind the leading edge of gas floodfront is recovered by the extraction mechanism, in addition to gravity drainage mechanism.

Further confirmations of these observations are obtained through the section-views of gas saturation, oil viscosity and oil saturation properties in these blocks. These are marked by 'star' symbol in **Figure 6-9A** through **Figure 6-9L** for the changes occurred in these properties right from start (1996) to the end (2126) of the secondary miscible CO_2 flooding process in Case-VII. Red numbers in on the right of the top-left figure indicates the oil zone layers, the target zone of the production in top-down process. Also shown are the injection and horizontal production wells (layer-8).

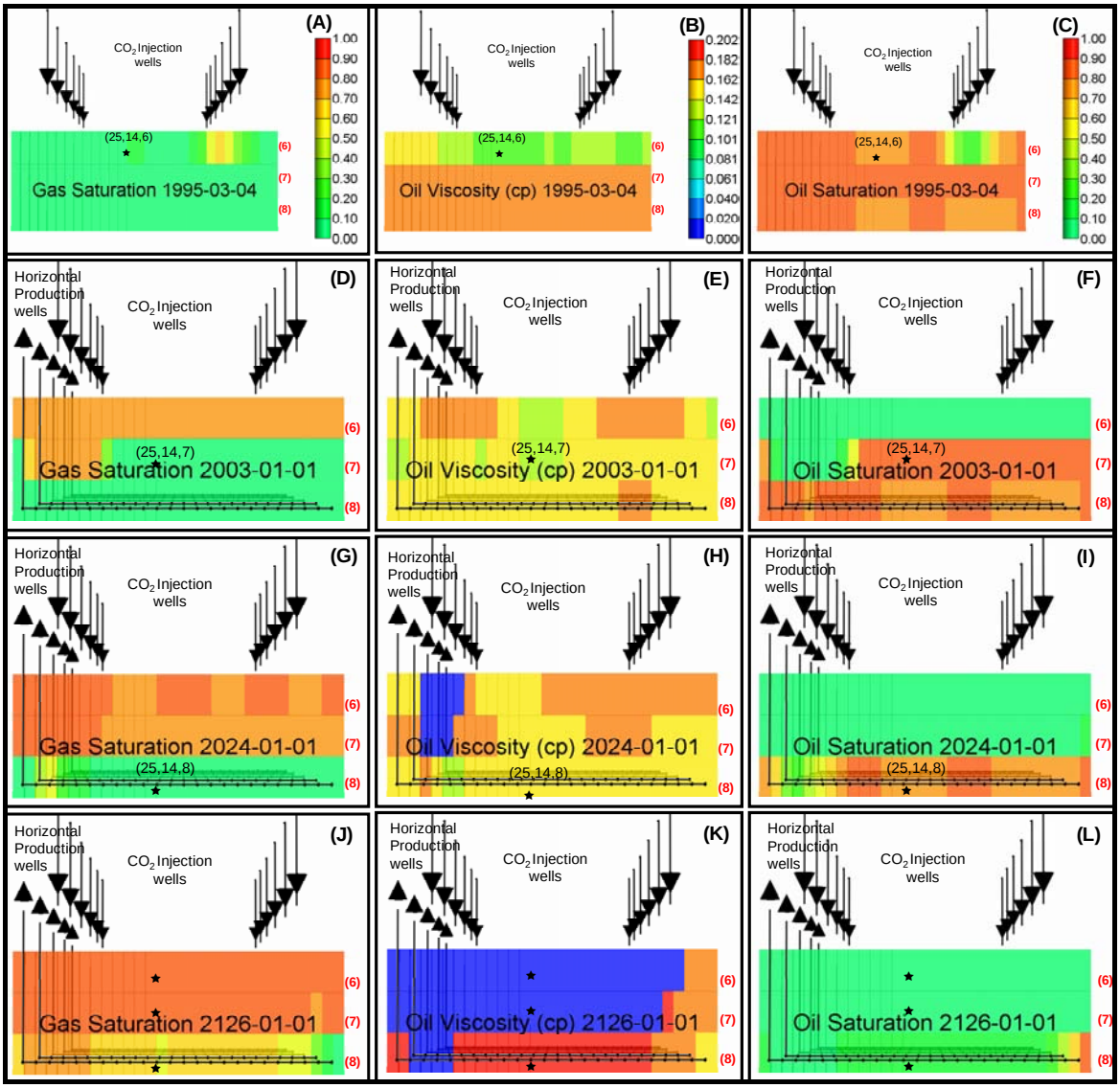

Figure 6-9: Oil recovery mechanisms other than the gravity drainage mechanism in blocks (25, 14, 6), (25, 14, 7) and (25, 14, 8) in top-down CO_2-assisted gravity drainage EOR process

Initial properties of the block (25,14,6) at the start of miscible flood in the year 1995 are as shown by star in **Figure 6-9A, 6-9B, and 6-9C**. As shown in **Figure 6-9D**, gas

saturation is increased to a value higher than 0.80 with the recovery of majority of oil (**Figure 6-9F)** through B-L type displacement. However, the respective oil viscosity in layer-6 is found to be increased indicating the extraction of the oil-components from this block (**Figure 6-9E)**. Gas floodfront reached block (25,14,8) by the year 2024 as shown in **Figure 6-9G,** which is then followed by the miscible front. With the continued production gas, oil viscosity in this year seems to be increased in some blocks, reduced, even to zero values, in some other blocks of layer-7 as well as the upper layer-6 (**Figure 6-9H)**. Zero values point out that the oil from these blocks has been completely recovered by the extraction of the oil-components behind the gas floodfront. Remember that the oil from these layers has not been completely recovered yet. **Figure 6-9J** shows that gas saturation increase did not achieve the values in the year 2126 of those observed in 2024 when the first gas breakthrough. Oil viscosity values reduced to zero in most of the layer-6 and layer-7 as shown in Figure 6-8K. It's values in the year 2126 reached to the values higher (in layer-8) than those observed earlier in 2003 and 2024. This demonstrates the ongoing process of the extraction during the downward movement of miscible zone while continuing to drain the oil under gravity drainage from the upper layer. Corresponding oil saturation at the end of miscible CO_2 flood is as shown in Figure 6-8L.

Figure 6-9 depict the changes in oil saturation in the block (21,20,7), overall reservoir pressure and GOR in case-V and VII well rate-constraint combination of the miscible CO_2-assisted gravity drainage EOR process during 132 years flooding.

In miscible process, the oil saturation in block (21,20,7) stays constant at 15 and 10 years in case-V (**Figure 6-10A**) and Case-VII (**Figure 6-10B**) respectively. Oil production occurred at the producing GOR equal to solution GOR which in turn represent the single phase flow. The respective pressure drop behaviour during this period suggests that the B-L type piston displacement of bulk-oil zone has occurred ahead of gas floodfront in secondary CO_2 injection. Once the bulk zone is produced, the leading edge of gas floodfront reaches the horizontal producing wells. It is marked by the sudden drop of oil saturation and respective rise in the GOR. Oil saturation gradually reduced to zero in 28 and 15 years in Case-V and Case-VII respectively. As discussed earlier, the miscible zone behind the CO_2 floodfront continue to extract the medium to heavy components of oil. This extracted oil drained under gravity. Related pressure changes in these 32 and 15 years are negligible (see section 6.1.1). Thus in turn satisfy the Cardwell and Parson's criteria of the downward free gravity drainage of oil from the reservoir.

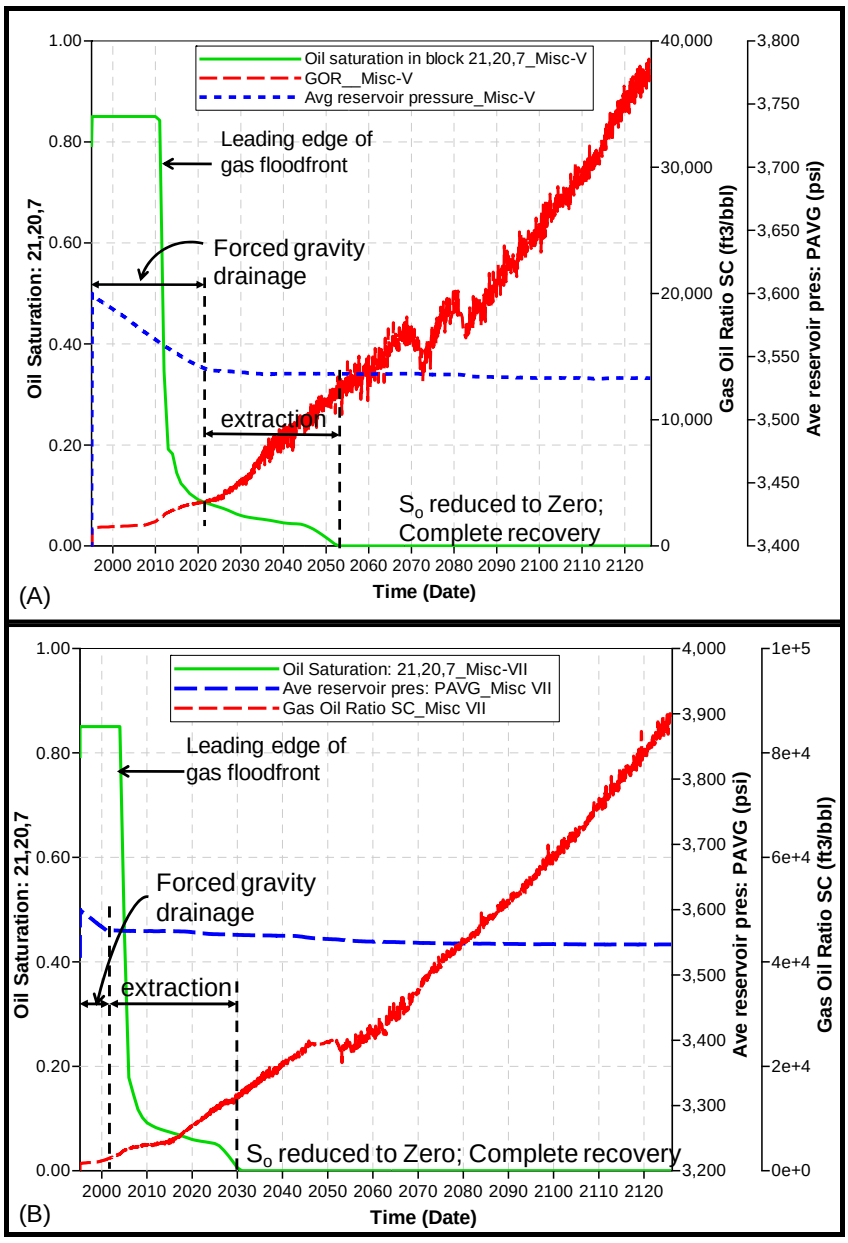

Figure 6-10: Miscible recovery contributing mechanisms in CO_2-assisted gravity drainage EOR process in the block (21,20,7)

Careful comparison of the micro-mechanisms contributing the forced and the free gravity drainage of the oil clearly point that the extraction mechanism in miscible flood recovers the same volume of oil in 32 and 15 years (**Figure 6-10**) compared to 125 and 64 years in the immiscible flood (**Figure 6-7**) from the block (21,20,7). These results clearly demonstrate that the extraction mechanism is much efficient mechanism that is capable of considerable faster oil recovery from the displaced oil-zone (behind the gas floodfront) compared to the oil film flow drainage mechanism in immiscible flood.

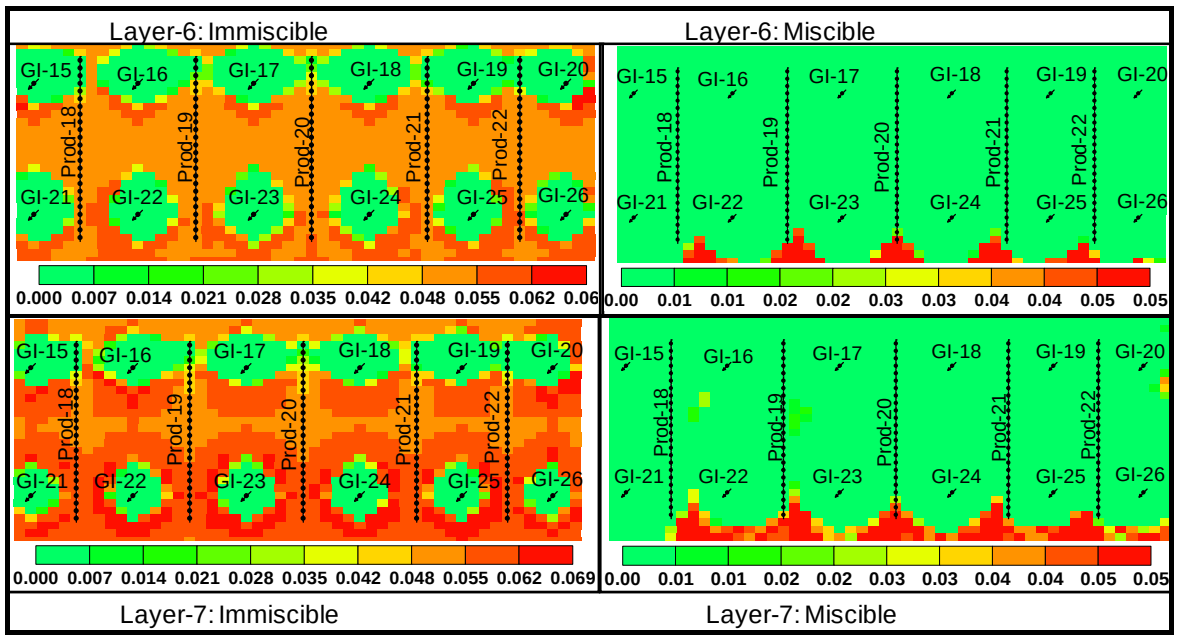

Figure 6-11: Comparative oil saturation in layer-6 and layer-7 (Areal view) in the year 2126 in immiscible and miscible flooding (Case-VII)

Figure 6-11 shows that the miscible mechanisms for Case-VII completely recover (mostly) layer-6 and layer-7 in the year 2126. Comparatively immiscible flood experienced very low oil saturation behind the gas floodfront. Conversely, these results again point out that the oil film flow under free gravity drainage in immiscible flooding is lower than the extraction mechanism in miscible flooding.

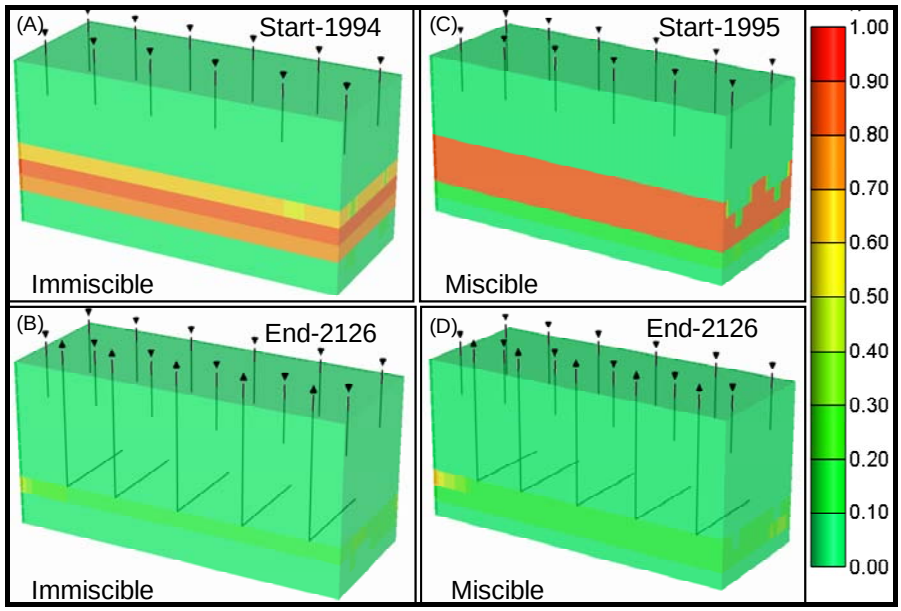

Figure 6-12: 3D representation of the oil recovered in immiscible and miscible process of Case-VII rate-constraint

Figure 6-12 shows that the oil saturation at the start of immiscible and miscible CO_2-assisted gravity drainage EOR process is produced mostly in 132 years of the CO_2 flooding (Case-VII). It is worthwhile to mention here that immiscible recovery in Case-VII yield 69% incremental oil recovery compared to 79% oil recovery in miscible process.

6.1.4 General Process Selection Map: Immiscible vs. Miscible CO_2-Assisted Gravity Drainage EOR Process

Results presented in section 6.1 concluded that the miscible flood yield higher recovery than the immiscible flood in CO_2-assisted gravity drainage EOR process. Moreover, the comparative incremental oil recoveries presented in Figure 6-1 demonstrate that the immiscible oil recoveries are higher than the miscible recoveries before gas floodfront arrival, whereas the miscible floods dominate later.

Ultimate incremental recoveries form the basis for the selection of either immiscible or miscible modes of CO_2 injection to obtain the optimized oil recovery. To achieve this, ultimate incremental recoveries of all the well rate-constraint combinations (Case-I to Case-VII) are plotted, as shown in **Figure 6-13**, vs. the respective incremental pore volumes of CO_2 injected.

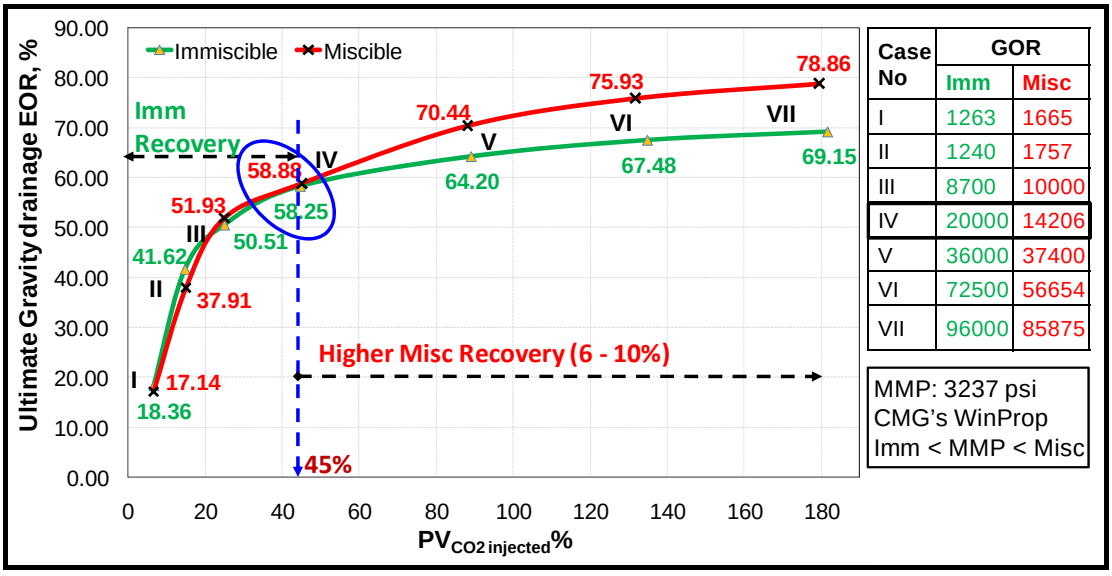

Figure 6-13: General selection map for immiscible versus miscible process - Case-I through Case-VII

Ultimate oil recovery pattern shows that immiscible recovery is high than miscible recovery by 1, 3.7, 1.5 for the pore volumes of 0.06, 0.15 and 0.25 in Case-I, Case-II and

Case-III respectively. Conversely Case-IV combination achieved nearly identical oil recovery for 0.45 pore volume of CO_2 injected (PV_{CO2}) in both the immiscible (58.25%) and miscible (58.88%) CO_2-assisted gravity drainage EOR processes.

For the remaining Case-V, Case-VI and Case-VII well rate-constraints combinations, this recovery pattern is reversed. Miscible recoveries are 70.44, 75.93 and 78.86% for Case-V, Case-VI and Case-VII respectively. On the other hand, those well rate constraint combinations yield the ultimate immiscible recoveries of 64.20%, 67.48% and 64.20% respectively. Associated pore volumes injected were 0.89, 1.34 and 1.82. These results show that miscible recoveries are higher than their immiscible counterparts by the 6.2, 8.5 and 10%.

At 0.45 Pore volumes of CO_2 injected, the ultimate incremental oil recoveries were identical in both the immiscible and miscible floods. This forms a distinction point for choosing between the immiscible and miscible process for a particular reservoir application.

From these results, it can be concluded that the immiscible CO_2 flood will yield higher or identical incremental oil recovery at a pore volume less than 0.45 PV_{CO2} injected (<45%). On the other hand, miscible flood will provide higher incremental oil recovery when the pore volumes higher than 0.45 PV_{CO2} are injected. This criterion can generally be used while selecting between immiscible and miscible CO_2 flooding process for the 50 API gravity Australian reservoir under investigation in this study.

Corresponding GOR values tabulated inside **Figure 6-13** show that GOR reach 20000 and 14000 in immiscible and miscible process for Case-IV well rate-constraint combination. It kept increasing in the higher combinations Case-V, Case-VI and Case-VII as 36000, 72500 and 96000 for immiscible flood and 37400, 56654 and 88875 for the miscible flood respectively.

GOR profiles show that the immiscible process GORs are higher than those observed in miscible GORs. As the reservoir oil is a very light oil of 50 ^{o}API gravity, the higher gas condensate production was observed at low pressure, immiscible flood. Conversely, high pressure gas injection recompresses gas in the reservoir. Moreover, the oil production is also controlled to maintain voidage balance. After leading edge of gas floodfront reached the drainage areas of the horizontal producing wells, miscible zone bind it maintains the reservoir pressure while continuing to extract oil from the displaced zone and draining under gravity.

In the recent years, governments limit the GOR values in an effort to reduce the atmospheric carbon emission. If the limit of the 20000 GOR is considered or assumed to be acceptable, then the corresponding recoveries, based on the selection criterion plot such as shown in the **Figure 6-13,** at 0.45 PV_{CO2} injected should be compared. Conforming to his argument, the immiscible and miscible recoveries at 0.45 PV_{CO2} injected are identical. Below this pore volume of CO_2 injected, immiscible process yield higher recovery recoveries (see **Figure 6-2, Figure 6-3** and **Figure 6-13)** are higher than the miscible recoveries. Furthermore, high pressure miscible CO_2 injection operations increase the cost of CO_2 compression, so the overall CO_2 flooding project. Considering the carbon emission and statutory limits on GOR, the immiscible CO_2-Assisted Gravity EOR process would be beneficial than the miscible gravity drainage EOR. Therefore, immiscible well rate-constraint combinations of Case-I to Case-IV should be selected for achieving the optimum oil recovery in the CO_2-assisted gravity drainage EOR process. Following this selection and complying with GOR limits, it can be concluded that the miscibility generation may not be a pre-requisite criteria for the optimum CO_2-assisted gravity drainage oil recovery.

6.2 Grid Refinement Studies: 50 ^{o}API Reservoir

Literature review presented in section 2.3.4.4 of Chapter-2 indicated the only one investigation for studying the effect of grid size by Fassihi and Gillham (1993). It further concluded that the effect of grid-thickness and grid-size on the CO_2-assisted gravity drainage oil recovery has not been so far investigated using CO_2 as the injection gas. This section is dedicated to establish effect of grid thickness and size in the miscible CO_2-assisted gravity drainage EOR process through compositional simulations on 50 ^{o}API gravity oil reservoir.

Results presented in the previous section using the base model (50 × 30 × 10: 600 × 400 × 150) concluded that the immiscible and miscible CO_2 injection over 132 years can obtain the optimum oil recovery of 69.15% and 78.85% respectively in the CO2-assisted gravity drainage EOR process. In order to explore further possibilities of achieving the incremental oil recoveries higher than these in relatively shorter operational time, the grid refinement studies are undertaken.

Two well rate-constraint combinations Case-VII and Case-IV (see **Table 6-1**) are used in this study. Results obtained in the base model of grid (50 × 30 × 10) with each

individual grid size (600 ft × 400 ft × 150 ft) in the earlier section are compared with the results obtained in the reduced grid thickness (layer) and grid size in this grid refinement studies. Details of these reduced grids and the parameters used in analysis are presented in **Table 6-2**. As Case-VII rate-constraint combination provided the highest incremental recovery, especially in the miscible flood, (see **Figure 6-13**), the results from this miscible Case-VII are presented first and then miscible Case-IV. The comparison parameter 'incremental EOR' is the percentage of oil recovered that was present in the reservoir at the start of secondary CO_2-assisted gravity drainage EOR flood.

Table 6-2: Details of grid thickness (layers) and grid size studies for both the Case-VII and Case-IV

Study parameters	Case	Number of grid blocks (i, j, k)	Grid dimensions (x, y and z)	Comments	Comparison parameters
Grid size	I	50 × 30 × 10	600 ft × 400 ft × 150 ft	Base Model	Incremental EOR, GOR and water cut vs. PV_{CO2inj}; and years of production
		50 × 30 × 10	**300** ft × **200** ft × 150 ft	x & y dimensions reduced	
	II	50 × 30 × **30**	600 ft × 400 ft × **50 ft**	Base Model	
		50 × 30 × 30	**120 ft × 80** ft × **50 ft**	x & y dimensions reduced	
Grid thickness	I	50 × 30 × 10	600 ft × 400 ft × 150 ft	Base Model	
		50 × 30 × **30**	600 ft × 400 ft × **50 ft**	Layer thickness reduced	

6.2.1 Effect of Grid Size (x and y-dimensions)

Grid size effect on the incremental oil recovery is studied in two reduced grid dimensions (x and y). In the first, x and y dimensions are reduced by half (300 ft × 200 ft) and one-fifth (120 ft × 80 ft) from the base-model dimensions (600 ft × 400 ft). Incremental oil recovery, GOR and water cut results are presented in **Figure 6-14** and **Figure 6-15**.

Figure 6-14A for Case-VII shows that the incremental recovery in the reduced size model (300 ft × 200 ft × 150 ft) is identical (79%) to the base model (600 ft × 400 ft × 150 ft) at the same 180 pore volumes of CO_2 injected. A similar identical oil recovery profile (60%) was obtained with Case-IV at 45% of PV_{CO2} injected. However, the respective GOR increased by 25000 (**Figure 6-14B**) and 5000 (**Figure 6-15B**) with the reduced grid size in Case-VII and Case-IV combination respectively. Water cut was 30% maximum in Case-

VII (**Figure 6-14C**) while no water production was observed with Case-IV (**Figure 6-15C**).

These results in both the well rate-constraint combination point out that the grid size has minimal effect on incremental recovery in the CO_2-assisted gravity drainage EOR process at reservoir scale. Similar results were presented by Fassihi and Gillham (1993) in air injection studies when they varied only the x-dimension length. The results on grid size Case-II are presented in the next section.

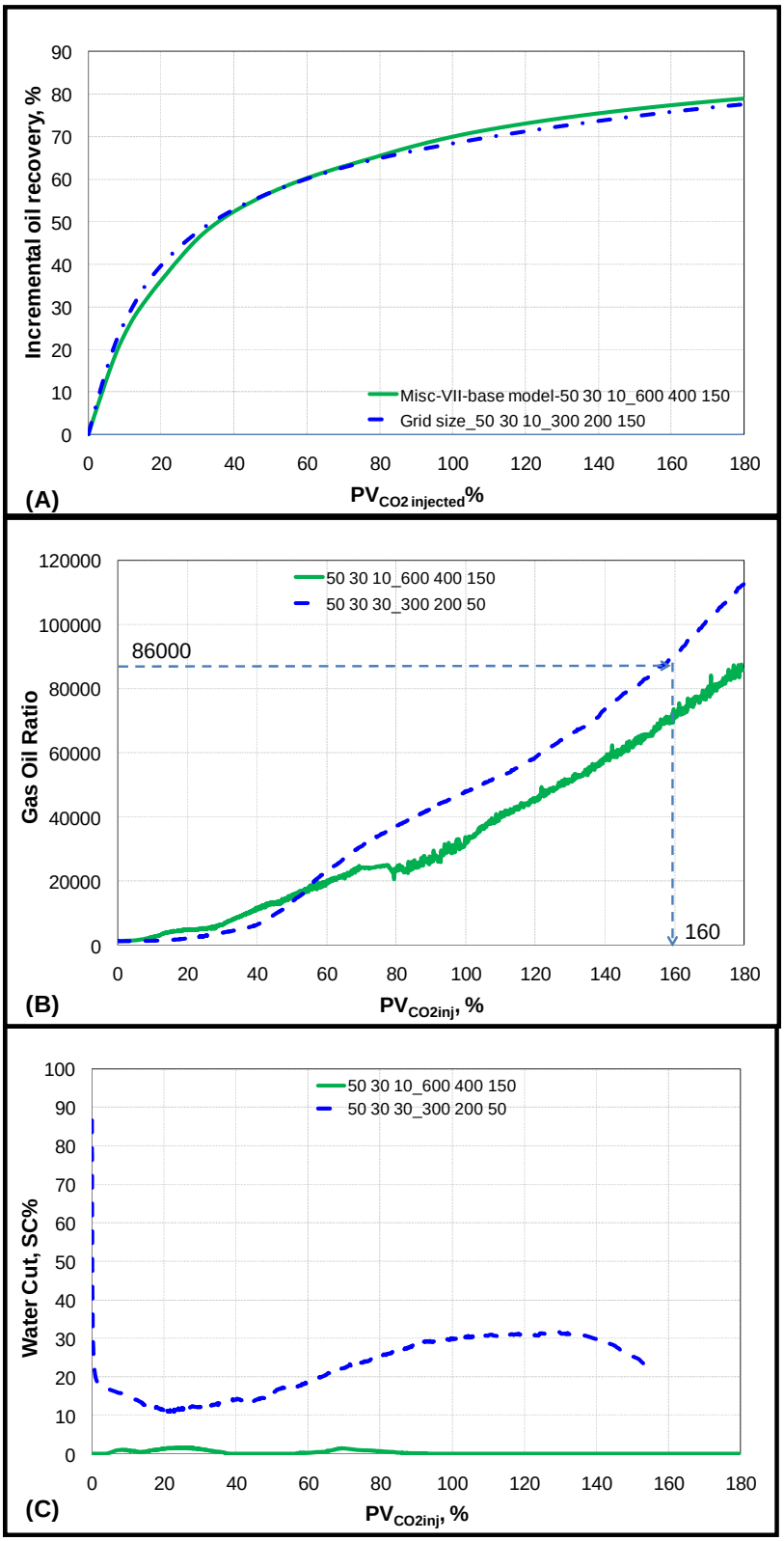

Figure 6-14: Effect of grid size on the incremental EOR, GOR and water cut, % in Case-VII

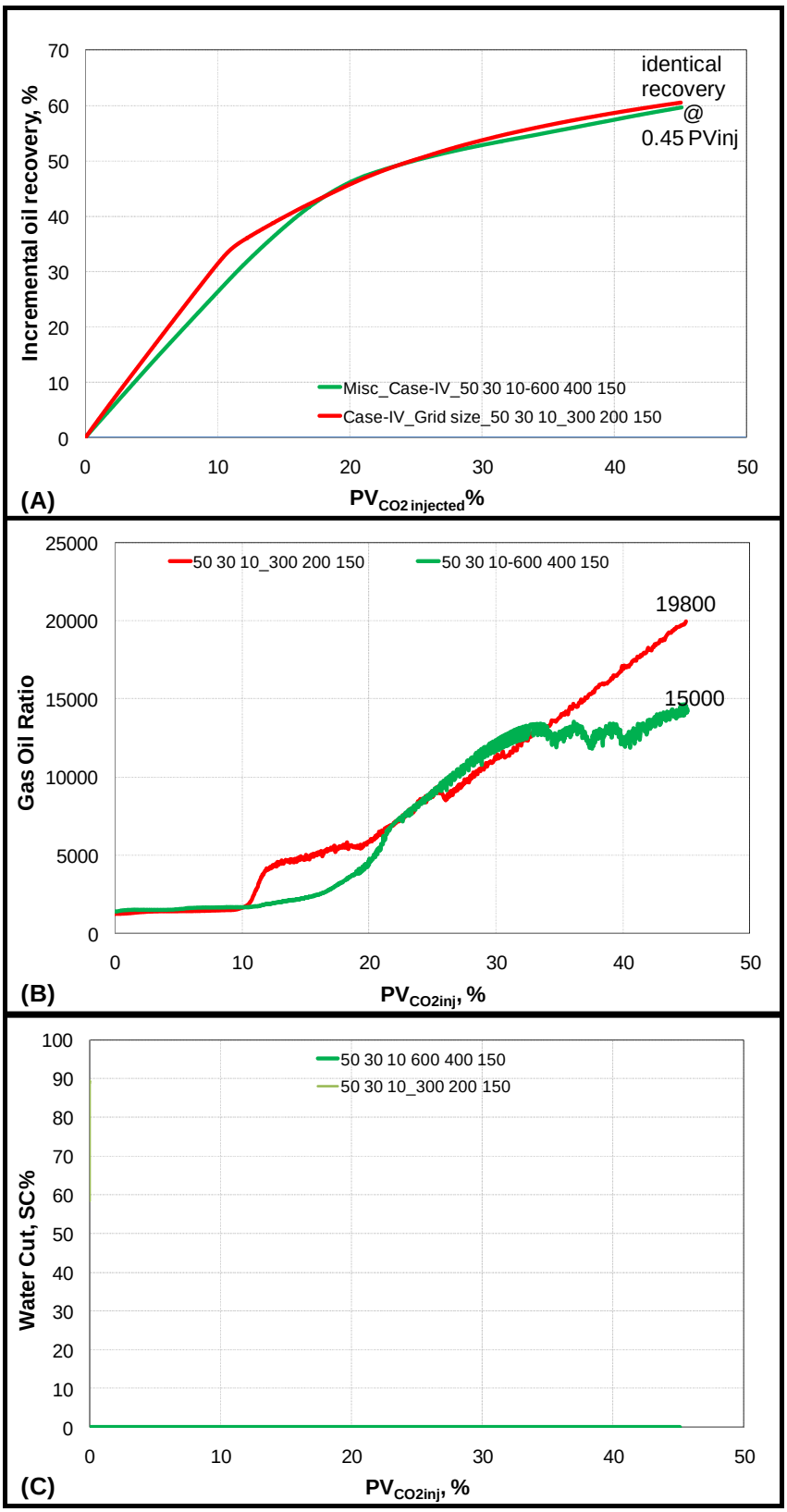

Figure 6-15: Effect of grid size on the incremental EOR, GOR and water cut, % in Case-IV

6.2.2 Effect of Grid Thickness (layer)

In this study, the layers in the vertical downward direction are increased by 3-times (30) from the base model layers (10) while reducing the layer thickness by one-third (50 ft) in both the Case-VII and Case-IV (see **Table 6-2**). This way the reservoir thickness along with the water, oil and gas zone is maintained same in order to compare its effect on the incremental oil recovery in the miscible CO_2-assisted gravity drainage EOR process. Horizontal production wells were recompleted in the layer 30 ft above the water-zone.

Results of the reservoir simulations regarding the grid thickness effect on CO_2-assited gravity drainage EOR process in Case-VII are shown in **Figure 6-16**. These results are compared at the 180% pore volumes of CO_2 injected, as represented in the base case model (see **Figure 6-13**). CO_2 injection started in March 1995. Within 24 years 180% pore volumes were injected in case of the reduced layer-thickness model (50 ft) in comparison with the 132 years in the base case model (150 ft). Incremental oil recovery increased by 6% (**Figure 6-16A**). Corresponding GOR at this pore volume was 1.08 E+05 (**Figure 6-16B**). If the incremental recovery is compared at the GOR level of base case model (86000), then 1% less recovery is obtained at 160% pore volumes. Water cut ranged between 20 to 40% in the reduced layer thickness model (**Figure 6-16C**). This could be because of closer 30 ft distance from the water-oil contact in comparison with the 75 ft in the base model ($50 \times 30 \times 10$: 600 ft × 400 ft × 150 ft).

On the other hand, the reduced thickness model yielded 10% higher recovery in 132 years for only 34% pore volumes injection (**Figure 6-17A)** in spite of the low well-rate combination (Case-IV). Moreover, the corresponding GOR (13000) was lower (**Figure 6-17B)**. Overall 16% higher recovery is obtained at 45% pore volumes of CO_2 injected (shown by red curve in **Figure 6-17A)** in comparison with the base case 180% PV_{CO2} injection. Water production was lower compared to the Case-VII.

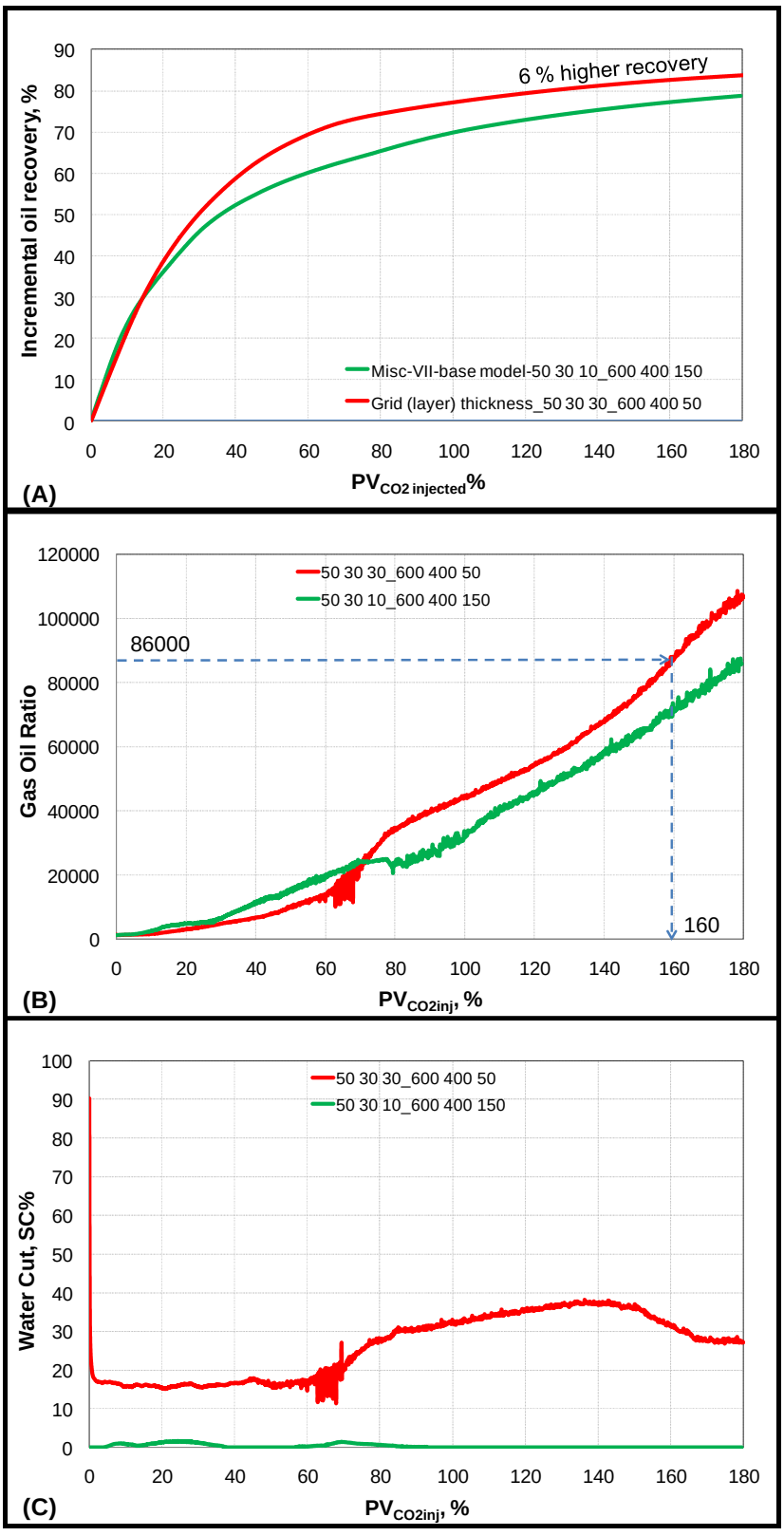

Figure 6-16: Effect of grid layer thickness on the incremental EOR (%), Gas-Oil Ratio (GOR) and water cut (%) in Case-VII well rate-constraint combination

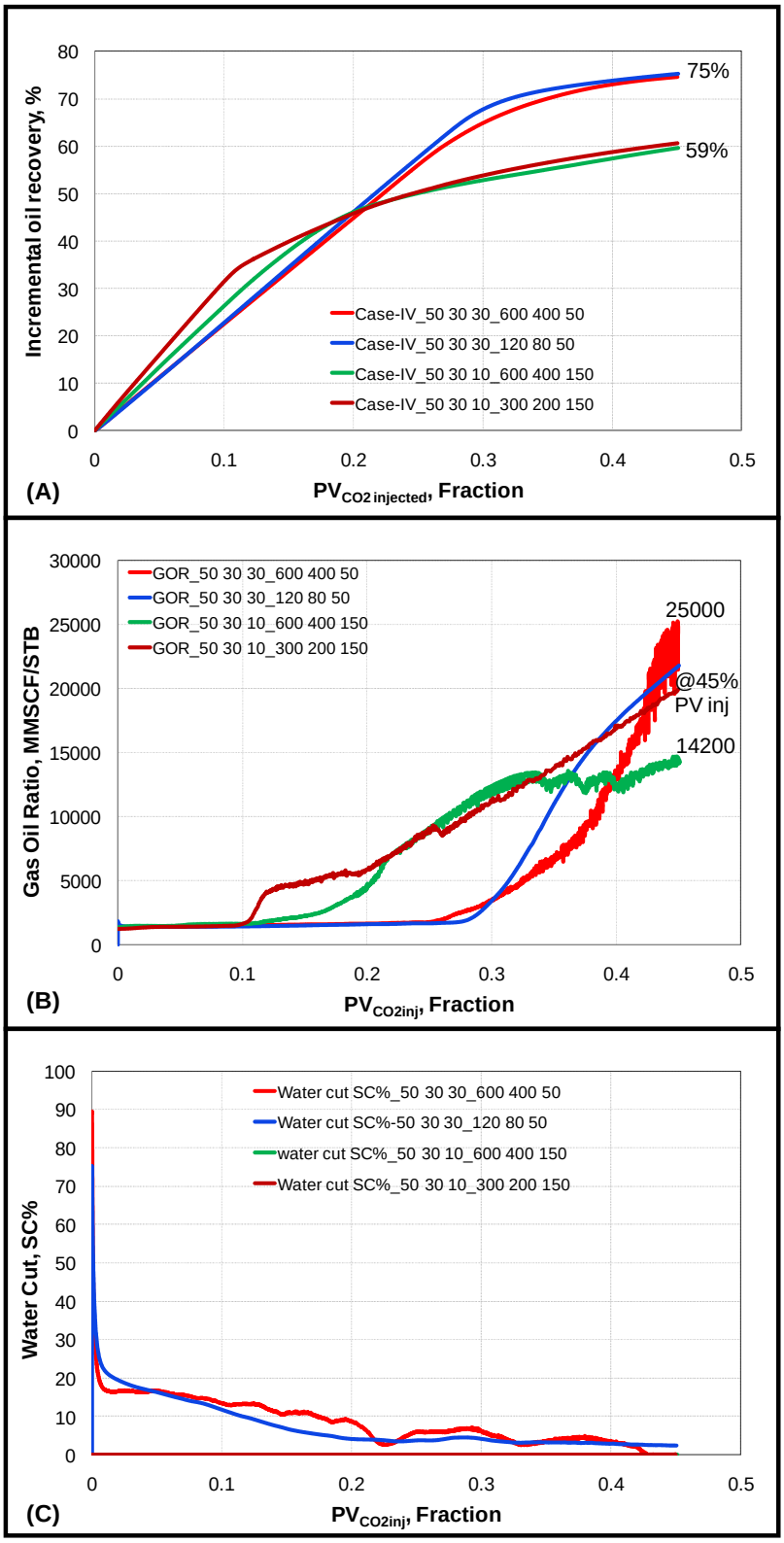

Figure 6-17: Effect of grid thickness on the incremental EOR (%), GOR and water cut (%) in Case-IV

These results in both the Case-VII and Case-IV point out that the smaller grid (layer) thickness models provide better incremental EOR profile at the lower pore volumes of CO_2 injected. It facilitates the effective drainage of oil that has been gravity-drained

from upper layers to the layers beneath. Moreover, the oil held up in these grid-blocks is prevented. This matters most especially in the layer in which the horizontal well is completed. On the other hand, Fassihi and Gillham (1993) and Ypma (1985) suggested that the bottom most layers should be thinner. Investigations in the current study concluded that thin layers facilitates the optimum gravity drainage oil recovery even in the upper layers, as indicated by the 6 (Case-VII) to 16% (case-IV) higher incremental EOR in case of the reduced thickness model (50 ft) compared to the base case model of 150 ft grid-thickness.

In both the Case-VII and Case-IV combination, CO_2 injection started in March 1995. For Case-VII, 180% pore volumes were injected within 124 years in case of the reduced layer-thickness model (50 ft) in comparison with the 132 years in the base case model (150 ft). On the other hand, 45% PV_{CO2} injection took 50 years more in reduced grid-thickness model than the base case model. This comparison shows that the lower well rate-constraint combination of Case-IV took 50 more years to inject 45% PV_{CO2}. While 4-5 times higher well rate-constraint combination of Case-VII takes only 8 years less for the injection of 180 PV_{CO2} in 132 years of miscible CO_2 flood. Subsequent incremental oil recoveries in Case-IV increased by 10% (34% PV_{CO2}) and 16% (45% PV_{CO2}) in spite of considerable low PV_{CO2} injection.

Keeping the grid thickness of 30 ft constant, grid size (x and y dimensions) is reduced by one-fifth, that is (120 ft × 80 ft) in the Case-IV well rate-constraint combination. **Figure 6-17A** (shown by blue curve) again shows that the incremental recoveries in this reduced model are nearly identical (75%) to the one obtained in base-case model (50 × 30 × 30: 120 ft × 180 ft × 50 ft). However, the reduced model recovered 75% incremental in only 8 years compared to 182 years in the base-model at the same 0.45 PV_{CO2} injected (See **Figure 6-17B**). In 132 years of miscible CO_2 flooding 8.9 PV_{CO2} was injected thereby recovering 98.4% incremental oil. At the injection of 2 PV_{CO2} in 30 years, the incremental oil recovery was 91.4%. Even at this level Final oil recovery is highly optimistic. Because of few years taken (30) comparatively to obtain the incremental recovery as high as 92%, it is concluded that the model, having grid-blocks (50 × 30 × 30) and grid size (120 ft × 180 ft × 50 ft) be adapted as “optimized grid-size model”. It thus provides the window of opportunity to study the full spectrum of the recovery profile even up to near-perfect recoveries. Therefore this model is referred as the “optimized model” (50 × 30 × 30: 120 ft × 180 ft × 50 ft) here onwards in this thesis and used in the further investigations.

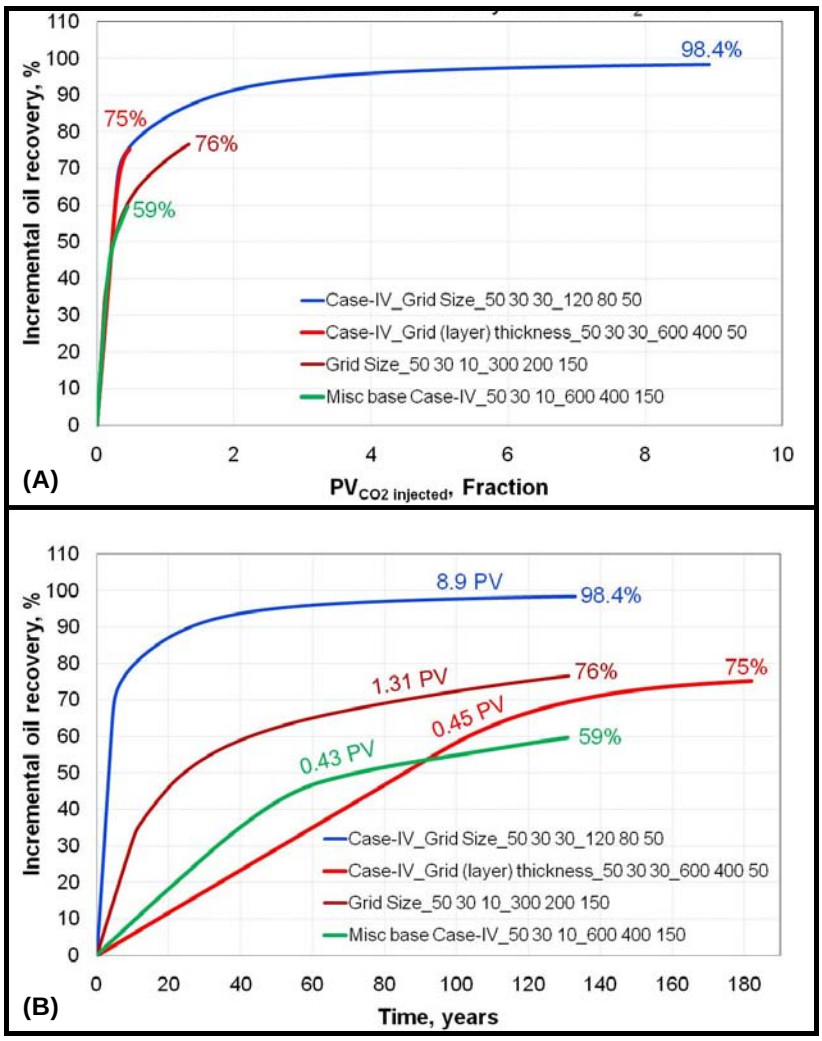

Figure 6-18: Incremental oil recovery (%) in the (A) respective pore volumes of CO_2 injected (fraction) and (B) years taken for this PV_{CO2} injection for all three grid sizes in Case-IV

6.2.3 Immiscible vs. Miscible Gravity Drainage Recovery with the New Optimized Grid (50 × 30 × 30: 120 ft × 80 ft × 50 ft)

The newly developed optimized grid (50 × 30 × 30: 120 ft × 80 ft × 50 ft) in the previous section, that yielded about 98.4% incremental oil recovery, is used in the comparative study of immiscible and miscible oil recovery in this section. **Figure 6-19** demonstrate the immiscible and miscible process performance over 132 years in Case-IV well rate-constraint combination.

Figure 6-19A shows that the incremental oil recovery in immiscible flooding keeps rising approaching towards the miscible process recovery with the final oil production rate of 157 (immiscible) and 42 (miscible) barrels per day. However the gas-oil ratio (GOR) is far higher than the miscible process. Water production is minimal in both the processes.

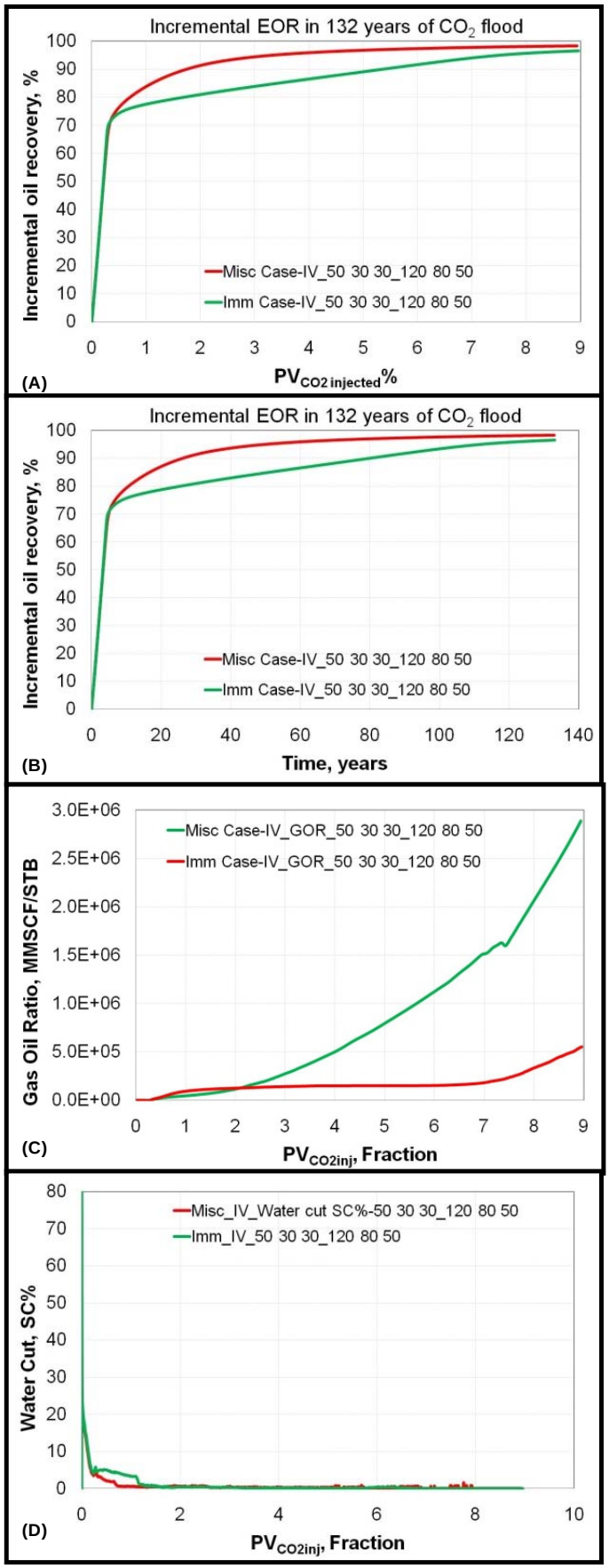

Figure 6-19: Immiscible vs. miscible process performance in CO_2-assisted gravity drainage EOR process (optimized grid: 50 × 30 × 30: 120 ft × 80 ft × 50 ft; k_v/k_h = 1.0)

Gas saturation, oil viscosity and the oil saturation profile changes in block (31, 14, 24) in both the miscible and immiscible process are shown in **Figure 6-20A** through **Figure 6-20D**. In miscible process, oil viscosity experienced swelling initially arising from its reduction, followed by its continuous increase until dropping to zero. This marks the complete oil recovery from the block (31, 14, 24) as shown in **Figure 6-14B**. During this process, the gas saturation also kept rising. This shows that the gas (that mostly contains CO_2) kept vaporizing the middle and heavier fractions of oil from this block until the complete recovery.

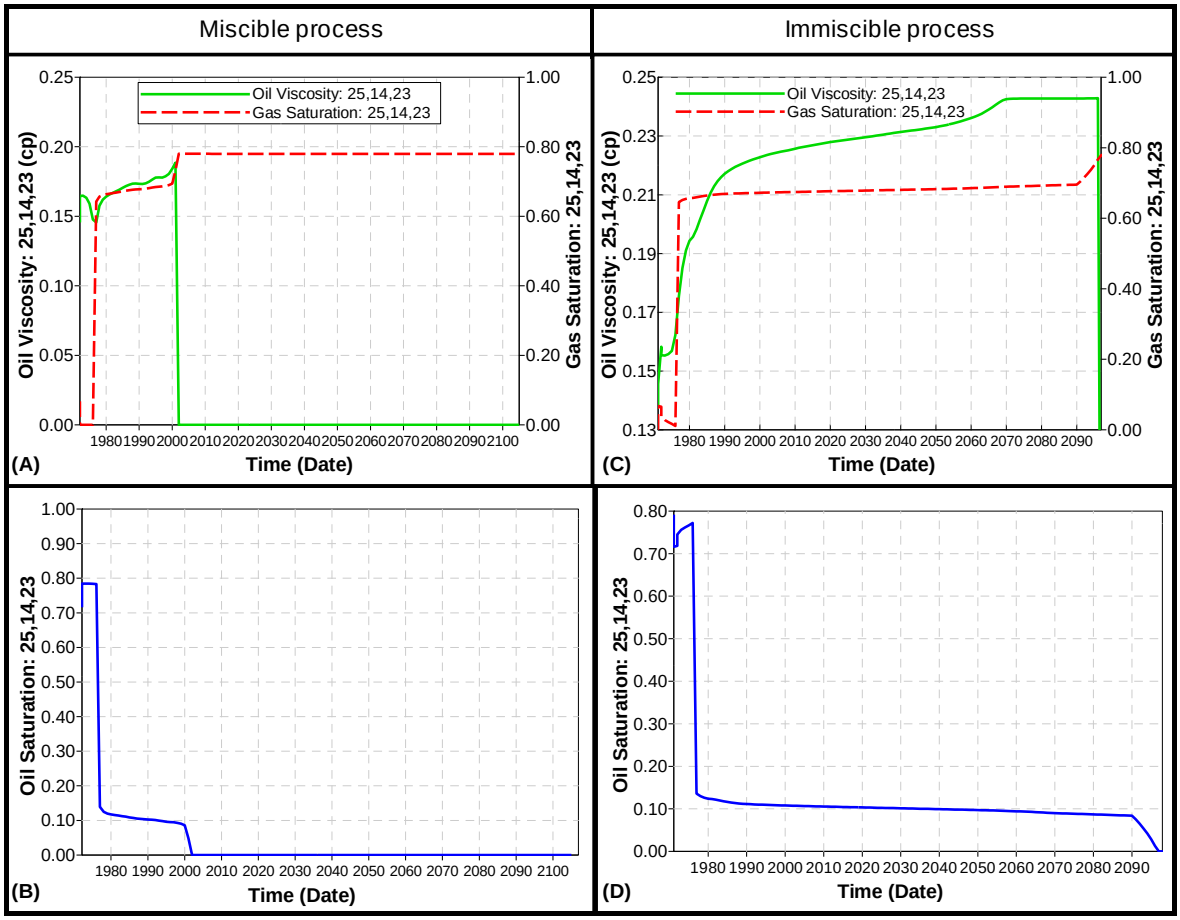

Figure 6-20: Mechanistic performance of the immiscible vs. miscible CO_2-assisted gravity drainage EOR process (optimized grid: 50 × 30 × 30: 120 ft × 80 ft × 50 ft; k_v/k_h = 1.0)

Immiscible process showed similar behaviour (**Figure 6-20C** and **Figure 6-20D**) indicating that CO_2 even in immiscible mode is capable of vaporizing the oil from the pores of the rock leading to the complete recovery. However, this oil viscosity increase is slow (near-flat curve in **Figure 6-20C**) in later stage in comparison with its sharp rise immediately after the CO_2 floodfront arrival (suggested by increase in the gas saturation in

this block. This slow oil viscosity increase profile combined with the slow oil film flow makes this immiscible oil recovery slower than the miscible recovery (see **Figure 6-20A** and **Figure 6-20C**). This is clearly evident from the oil saturation profiles shown in **Figure 6-20B** and **Figure 6-20D** wherein complete oil recovery took place in only 30 years (from February 1972 to January 2002) compared to 124 years (in the year 2097) in immiscible process from the representative block (25, 14, 23).

Reservoir pressure changes are depicted in **Figure 6-21** in both the immiscible and miscible process. In immiscible process the reservoir pressure dropped by 100 psi in 16 years (6psi/year) until arrival of the CO_2 floodfront (CO_2 breakthrough) in 1988. On the other hand, this pressure drop was higher in the miscible process. It dropped by 14 psi/year for 10 years until the gas floodfront arrival in 1982. This reservoir pressure behaviour indicates that the recovery mechanism until this phase of the production remained Buckley-Leverett type of displacement.

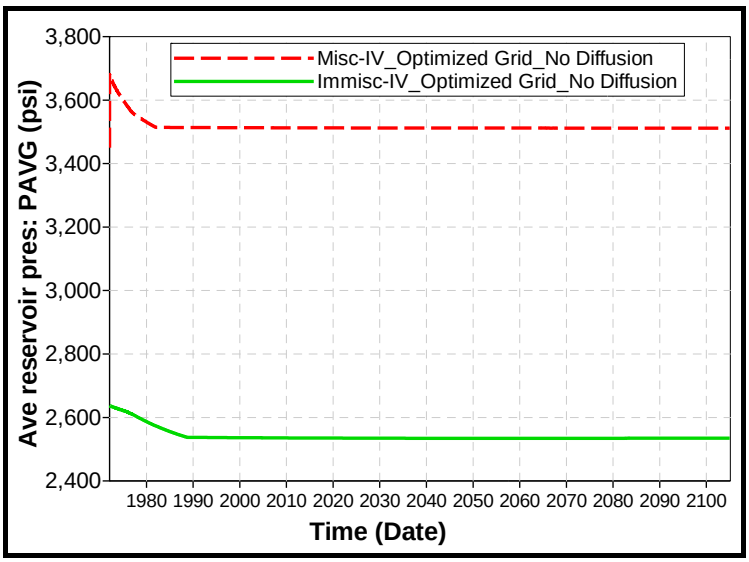

Figure 6-21: Average reservoir pressure in immiscible and miscible CO_2-assisted gravity drainage EOR process (optimized grid: 50 × 30 × 30: 120 ft × 80 ft × 50 ft; k_v/k_h = 1.0)

Once the leading edge of the gas floodfront reached the producing horizontal wells and the gas (that mostly contains CO_2) breakthrough occurred, the recovery mechanisms differ. In immiscible process, oil film flow is supported by the vaporization of middle and heavier fractions of the oil from the pores behind gas-oil contact, especially with CO_2 as an injection gas. Miscible process is governed by the vaporization of the oil (including heavier fractions) from the pores behind the miscible zone is the main recovery mechanism after

the gas breakthrough. Reservoir pressure remained constant thereafter in both the immiscible and miscible process.

6.3 Effect of Heterogeneity

In CO_2-assisted gravity drainage EOR process, CO_2 is injected in the gas-cap in the layer just above the oil zone which then slowly drives the GOC vertically downward to facilitate the oil-drainage under gravity effect. Because of this process mechanism, the formation characteristics such as vertical permeability (k_v/k_h ratio) and the porosity variation with increasing depth especially in the successive oil bearing target zones play important role in the outcome of the EOR operations. In this investigation, effects of these two parameters are studied by varying vertical permeability from 1200 mD to 1.2 mD (50 ^{o}API gravity oil and the compositional simulation) and the porosity increasing with the increasing depth in the oil zone (35 ^{o}API gravity oil and the pseudomiscible simulation).

6.3.1 Permeability Heterogeneity

Comparative recovery performance in miscible CO_2-assited gravity drainage EOR process over 132 years is represented in **Figure 6-22**. 94% incremental oil was recovered in 40 years of the miscible CO_2 flooding since its start in 1972 when the vertical permeability of the reservoir was kept 1200 mD (k_v/k_h=1.0). However the incremental recovery curve flattened thereafter leading to the final recovery of 98.4% (**Figure 6-22**A). **Figure 6-22B** shows that 9 Pore volumes of CO_2 were required to be injected to achieve this recovery.

On the other hand, incremental oil recovery was 18% lower (76%) when the vertical permeability was kept 1.2 mD (k_v/k_h=0.001) compared to 1200 mD vertical permeability reservoir (k_v/k_h=1.0). Incremental recovery kept rising in contrast with flattened curve in their counterparts (1200 mD reservoir). Low permeability reservoir yielded 95.5% incremental recovery, 3% lower than the 1200 mD reservoir (**Figure 6-22**A). Moreover, lower permeability reservoir (1.2 mD) needed only 3 Pore volumes of CO_2 to be injected (6 less pore volumes of CO_2) in yielding 95.5% recovery (**Figure 6-22B)**.

Gas-oil-ratio (GOR) comparison in **Figure 6-22C** show that the 1.2 mD reservoir exhibited low gas production with GOR of 70000 MMSCFD/STB in comparison with the

2.8E+06 MMSCFD/STB in the 1200 mD reservoir. Water production in the 1.2 mD vertical permeability reservoir was higher (maximum of 10%) until gas floodfront arrival in 1992, which then reduced to a level of 1200 mD permeability reservoir (**Figure 6-22D**).

In CO_2-assisted gravity drainage EOR process, highly compressible CO_2 is injected in the gas-cap to assist the gravity drainage of the oil in the oil zone downward towards the horizontal producer placed at 30 ft above the water-zone. However, oil-drainage in the low permeability nature of the formation (such as in the case of kv/kh ratio of 0.001) is slower than the drainage in the higher kv/kh ratio 1.0. Due to the lower downward-Darcy velocity, gas floodfront advancement, hence its spreading will also be slower. This helps to maintain the average reservoir pressure with minimum drop as demonstrated in **Figure 6-23**. This, in turn, creates a constant pressure profile behind the CO_2 floodfront in the gas-cap, thus satisfying the essential condition of the Cardwell Parsons (Cardwell and Parsons, 1949b). The results presented in **Figure 6-23** suggests that the gravity drainage mechanism in permeability-heterogeneity reservoir (lower k_v/k_h ratio such as 0.001) is more of the free rather than the forced gravity drainage mechanism as suggested in the high vertical permeability (1200 mD) reservoir.

Moreover, CO_2 will exhibit the tendency to disperse in the horizontal direction through the tortuous porous media due to the higher horizontal permeability (in low kv/kh reservoirs) at the gas-oil interface. The slower downward movement of GOC because of the low oil-drainage rate, the CO_2 will have more time to diffuse through the oil phase across the interface. This leads to the “active diffusion phenomenon” which further helps in the efficient vaporization or extraction of the oil from the pores. Gas diffusion effect is investigated in the next section.

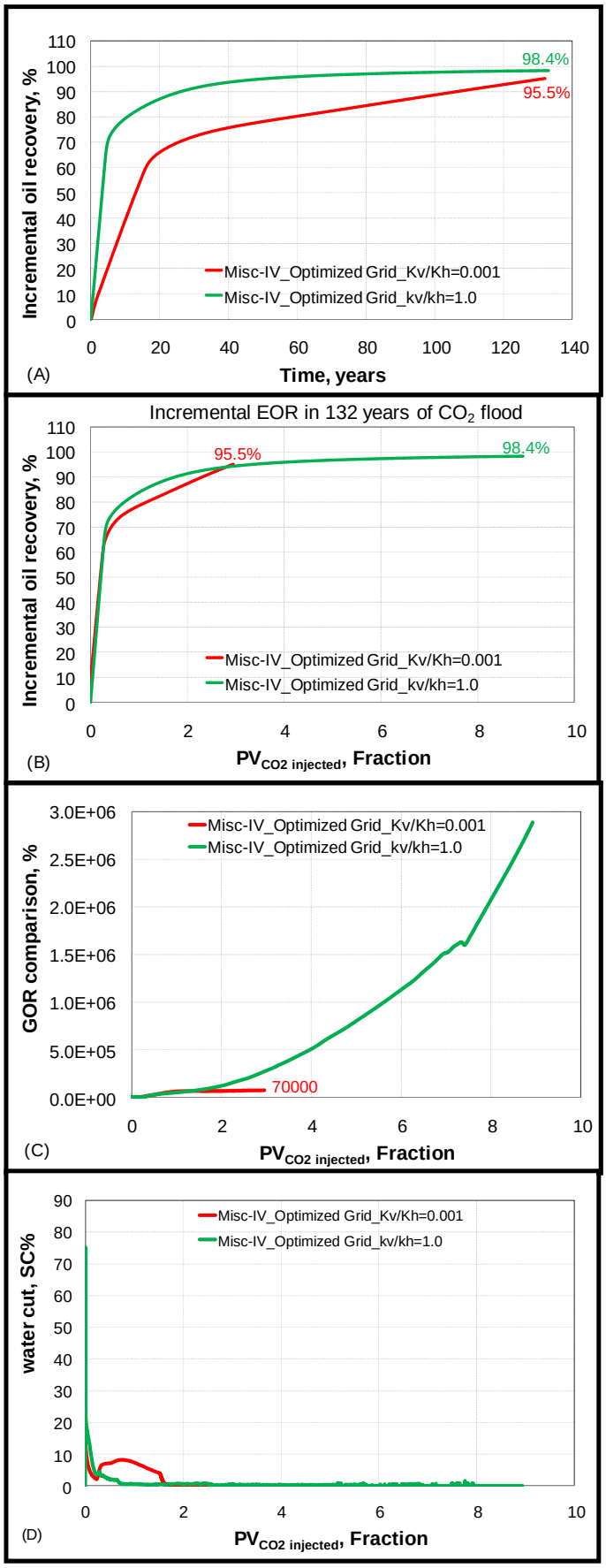

Figure 6-22: Comparison of permeability heterogeneity (k_v/k_h = 1.0 and 0.001) effect on performance of *miscible* CO_2-assisted gravity drainage EOR (optimized grid: 50 × 30 × 30: 120 ft × 80 ft × 50 ft)

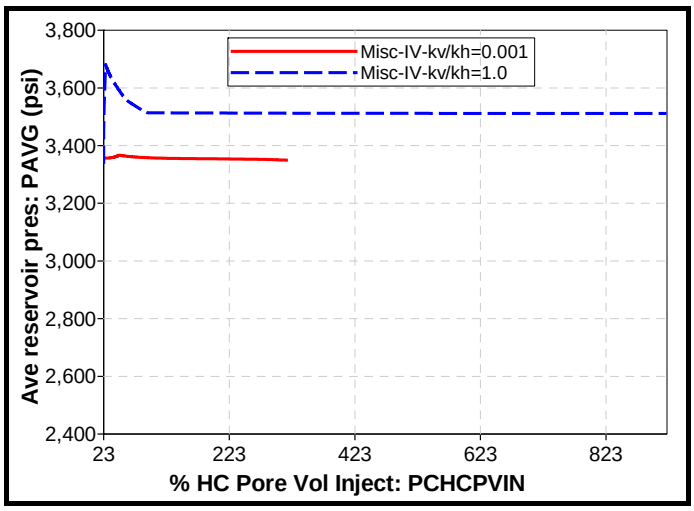

Figure 6-23: Average reservoir pressure in miscible CO_2-assisted gravity drainage EOR process in homogeneous (k_v/k_h = 1.0) and heterogeneous (k_v/k_h = 0.001) reservoir (optimized grid: 50 × 30 × 30: 120 ft × 80 ft × 50 ft)

6.3.2 Porosity Heterogeneity

Porosity heterogeneity effects on the CO_2-asssited gravity drainage EOR process on 35 ^{o}API reservoir. Pseudomiscible black-oil model using CMG's IMEX simulator was used in these simulations in irregular well patterns.

Two sets of porosity values (**Table 6-3**) were used in this study. In the first (Set-I), uniform porosities are assigned in oil zone (0.22) and water zone (0.18) while it is assumed increasing downwards in gas zone. Water zone has a lower porosity than the upper oil zone. In second setting, porosity of the formation is increasing downwards from the top layer. Gas injection and oil production rates used are 67.5 MMSCF/D and 13000 bpd respectively. Results obtained in these setting are then compared to the results obtained in the homogeneous porosity (0.22) setting of Case-III (see Case-III in **Table 5-1**).

Table 6-3: Porosity heterogeneity settings

Layer	Set-I	Set-II
1	0.17	0.14
2	0.18	0.16
3	0.19	0.18
4	0.2	0.19
5	0.22	0.2
6	0.22	0.22
7	0.22	0.22
8	0.18	0.28
9	0.18	0.38
10	0.18	0.42

Lowest oil production is obtained in setting-I of the three porosity settings (**Figure 6-24**). Respective cumulative oil production is also lowest and the decline of oil production rate is higher in Setting-I in comparison to the homogeneous reservoir (porosity of 0.22). However, CO_2 breakthrough at horizontal production wells is delayed by 4 years against the homogeneous porous media settings. Corresponding oil recovery is prolonged by 4 years before declining in 2084. Most of the oil in layer-6 was drained by gravity in year 2100. Noticeably highest GOR (25000 cu ft/bbl) and WOR (higher than 1.2) values were obtained in setting-I.

In Setting-II, more stable and higher oil production rates are observed as shown by the flattened curve. CO_2 breakthrough occurred 3 years earlier than setting-I and 4 years later than the homogeneous setting. Even after CO_2 breakthrough has occurred, oil production rates are higher in comparison to the homogenous porosity setting (Case-III of Table-2) and Setting-I. GOR of 16000 cu ft/day and WOR of 0.3 are the lowest values observed amongst these settings. Cumulative oil recovery is higher than the other two settings.

EOR mechanism is similar to that observed in rate sensitivity studies. Before CO_2 breakthrough, the reservoir was produced with the producing GOR is equal to solution GOR. After CO_2 breakthrough GOR sharply increased. Before and after CO_2 breakthrough, an average reservoir pressure drop of maximum 10 psi was observed during 98 years of oil recovery. This suggests the EOR mechanism to be the CO_2-assisted gravity drainage mechanism.

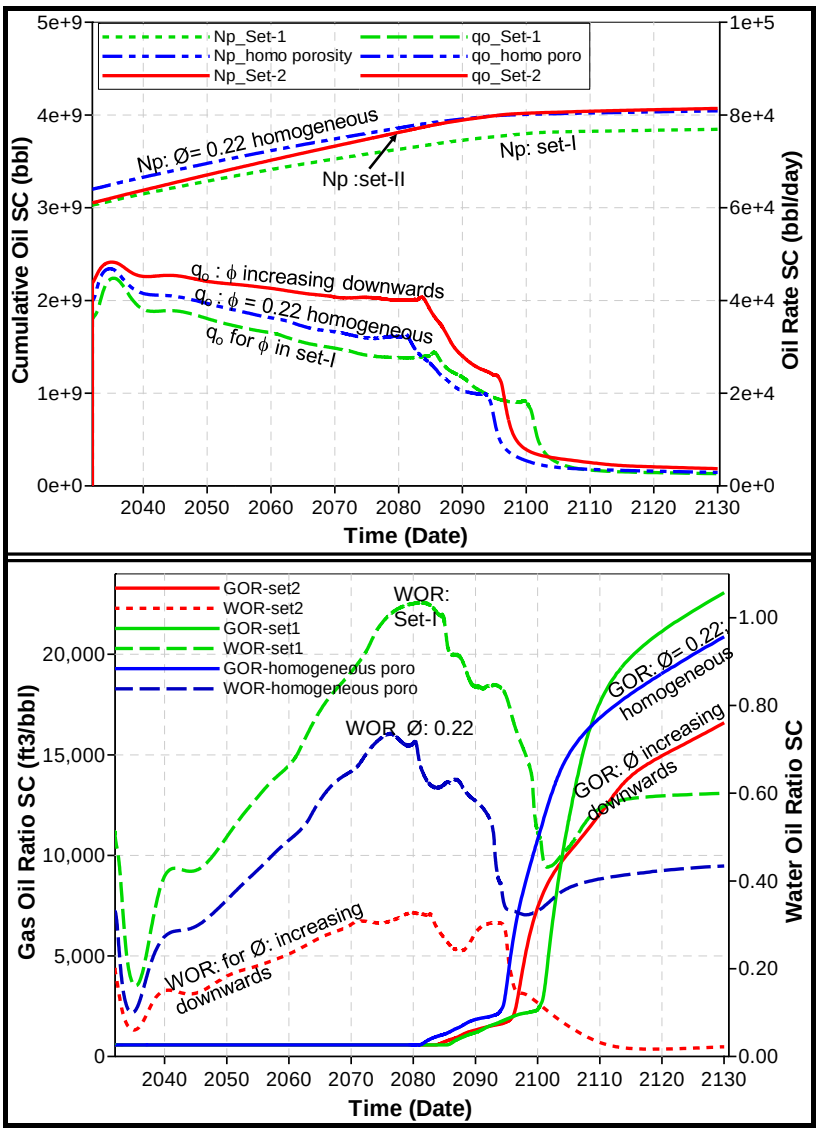

Figure 6-24: Effect of porosity heterogeneities on CO_2-assisted gravity drainage EOR performance in set-I & set-II compared to base Case-III

These results of porosity heterogeneity studies point out that the reservoir with porosity increasing downwards is favoured in GAGD-EOR process than the other porosity heterogeneity setting. This is evident from **Figure 6-25** wherein the increased oil saturation in layer-7 is more in Setting-II (porosity increasing downwards) compared to Setting-I. It is due to fact that the increasing pore volume, so the porosity in setting-II improves the sweep efficiency and efficient downward oil drainage under gravity effect.

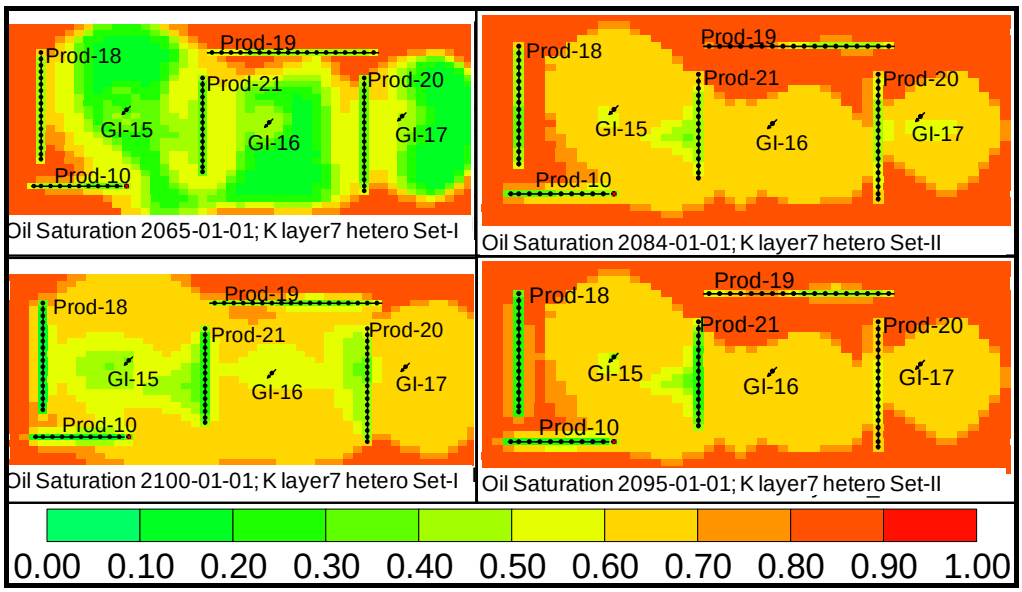

Figure 6-25: Effect of porosity heterogeneity on CO_2-assisted oil gravity drainage oil recovery in Setting-I and Setting-II

6.4 Effect of Molecular Diffusion/Dispersion

Effect of the molecular diffusion is investigated through the compositional simulations over the optimized grid of size (50 × 30 × 30: 120 ft × 180 ft × 50 ft) in Case-IV combination. Diffusion phenomenon is simulated using Sigmund correlations in both the homogeneous and heterogeneous reservoir having k_v/k_h ratio equal to 1.0 and 0.001 respectively. These simulations are conducted using the optimized grid and the 50 ^{o}API oil. No-diffusion results are then compared with the diffusion case results.

6.4.1 Homogeneous Reservoir (k_v/k_h = 1.0)

Vertical permeability is kept uniform as 1200 mD equal to horizontal direction permeability. Simulation results obtained in this case are as presented in **Figure 6-26. Figure 6-26A** clearly demonstrates the importance of diffusion phenomenon that significantly yielded 12% higher incremental oil recovery at the 1.45 PV_{CO2} injected. Moreover it exhibited near-perfect recovery in the optimized grid. Gas production is also lower compared to the no-diffusion case. Gas-Oil ratio profiles (**Figure 6-26C)** further suggest that the diffusion phenomenon do not start until the CO_2 floodfront arrival (CO_2 breakthrough). CO_2 breakthrough is delayed in the diffusion case in comparison with the no-diffusion case. It is further confirmed by 3 years delay (January 1980 instead of January 1977 in the no-diffusion case) in the start of gas saturation rise in the block (21, 14, 24) representing the reservoir section at the bottom of the oil zone as shown in **Figure 6.27A**

and **6.27C**. Concentration gradient driven diffusion of CO_2 in the oil phase leads to oil-swelling (with minor oil vaporization) depicted by the viscosity reduction. However, this oil swelling is only at the floodfront in case of the no-diffusion case. This causes increase in oil mobility which further helps in the effective gravity drainage of the oil (see **Figure 6.27B** and **Figure 6.27D**). Miscible oil recoveries start to deviate from this point onwards (**Figure 6.26A**).

After gas (which mostly contains CO_2) floodfront arrival (in January 1980) in the block (21, 14, 24), minor reduction in the oil viscosity is observed from 0.141 cP to 0.139 cP with the respective reduction in the oil saturation from 0.668 to 0.532 for a year. Consequently oil mobility increased at the front owing to the oil swelling. Beyond January 1981, oil viscosity trend is reversed leading to its increase to 0.155 cP in 3 years. During same period, gas saturation continued to increase, which began since CO_2 floodfront arrival. This means that the CO_2 starts to vaporize the light-intermediate components of the oil from this block (21, 14, 24) causing oil to shrink thereby reducing the viscosity. This process is continued until all of the oil in the block (21, 14, 24) is completely recovered in January 1999, as shown in **Figure 6.27D**.

The respective oil saturation (**Figure 6.27D**) in this block exhibited its increase from January 1983 to 1986 and then January 1987 to 1989. CO_2 vaporizes the oil from the pores behind the floodfront from the upper layers, which is then gravity drained downwards in this block until diffusion and oil vaporization process from upper blocks is complete. Similar observations were noted in other blocks of the reservoir. In later stage, CO_2 vaporizes the heavier fractions of oil. Therefore this result point out that the diffusion induced oil vaporization must be accompanied by gravity drainage of oil from upper blocks to downward blocks leading to the flow in the horizontal wells.

Moreover, the diffusion and oil-vaporization mechanism further appears to hasten the oil recovery process. With the diffusion case, CO_2-assisted gravity drainage oil recovery process from this block and so the reservoir completed in 26 (**Figure 6.26B** and **Figure 6.27D**) and 22 years respectively. On the other hand, no-diffusion case took 58 years to completely recover the oil. These finding further exemplifies the importance of the diffusion mechanism in the CO_2-assisted gravity drainage EOR process.

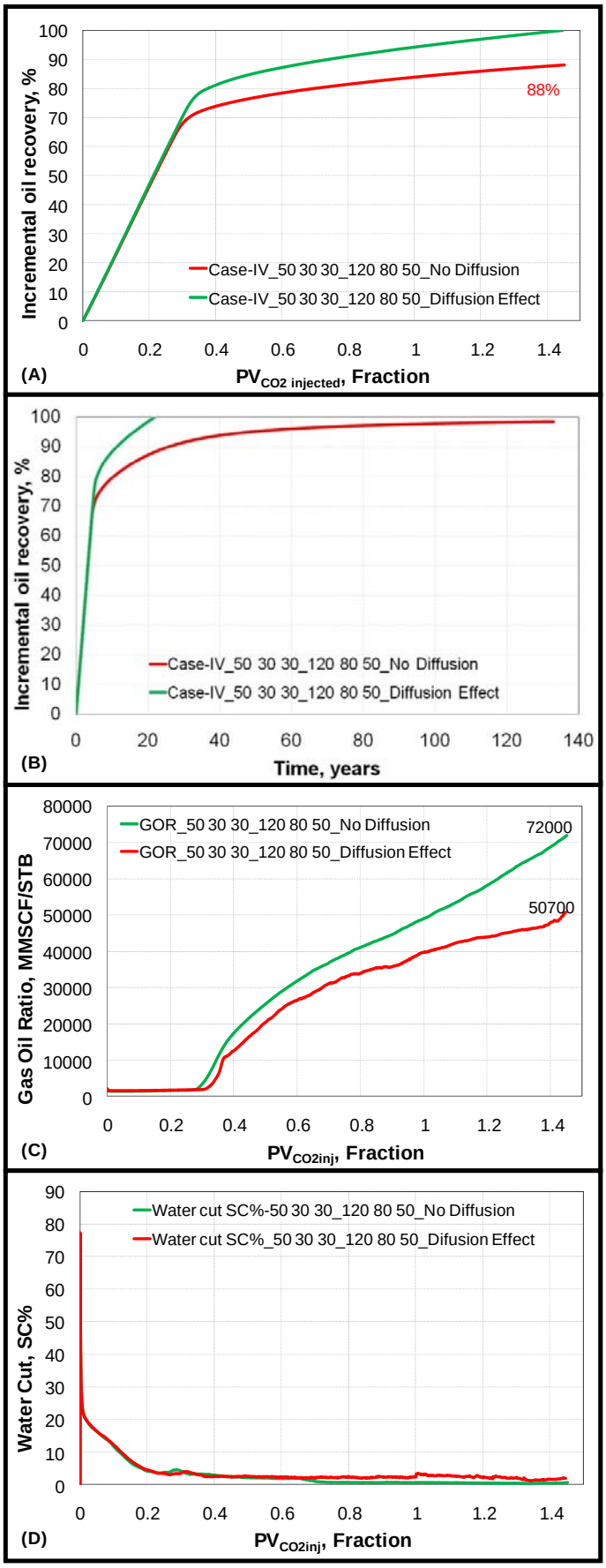

Figure 6-26: Effect of molecular diffusion in miscible process (Case-IV; optimized grid: 50 × 30 × 30: 120 ft × 80 ft × 50 ft; k_v/k_h = 0.001)

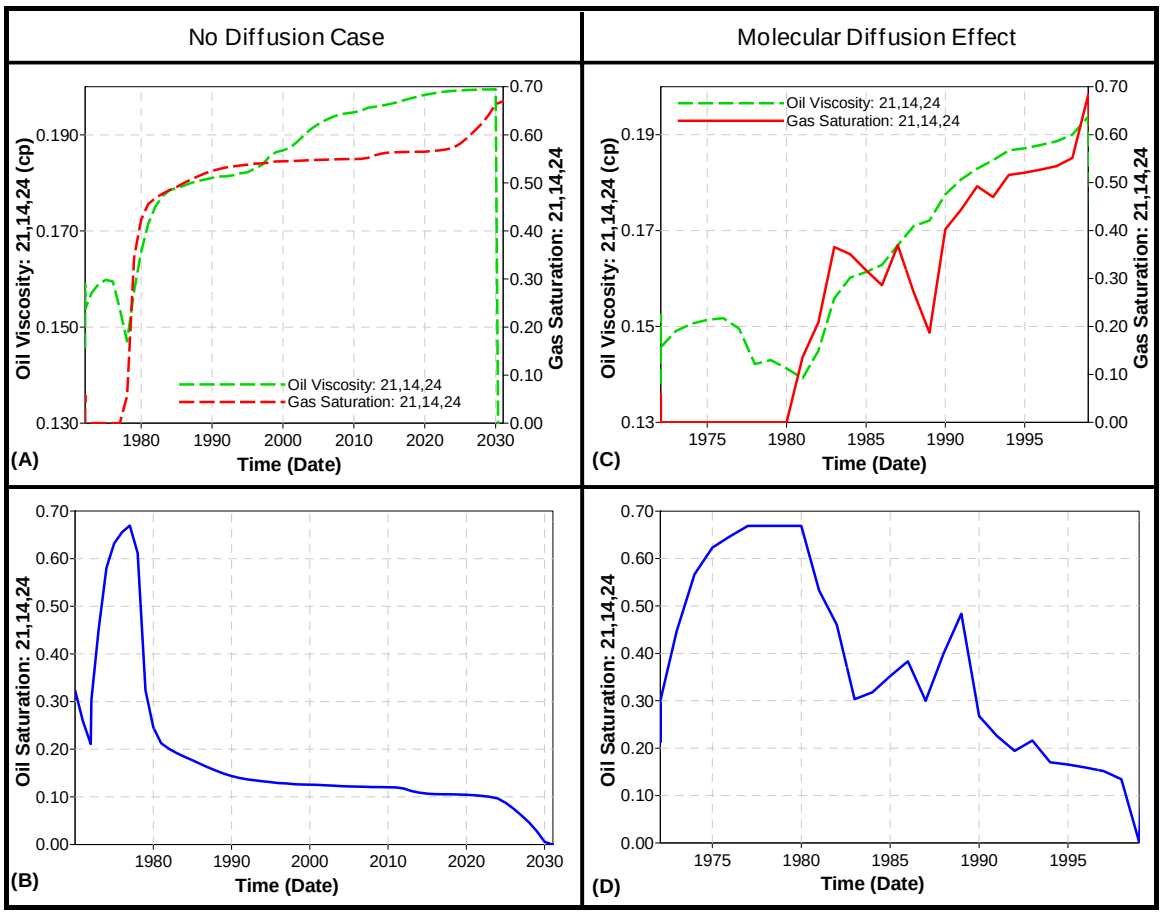

Figure 6-27: Effect of molecular diffusion in the miscible process (Case-IV) using optimized grid (k_v/k_h = 1.0); Gas saturation, oil viscosity and saturation at the middle of 24th layer block (21, 14, 24)

Results presented in section 6.2.3 indicated from the viscosity increase profile (along with the gas saturation and oil saturation profiles in **Figure 6-20**) that CO_2 vaporizes the left-behind oil residing in the pores behind CO_2 floodfront. Continuous, but steady, increase in the oil recovery hinted at the slow diffusion process even in immiscible CO_2 injection. Figure 6-28 represents the effect of diffusion on the incremental oil recovery in immiscible process. Immiscible process without diffusion yielded 96.63% final incremental recovery for 8.9 pore volumes of CO_2 injection at the end of 132 year CO_2 flooding (**Figure 6-28A**). Conversely, diffusion mechanism recovered the nearly same volume of incremental oil in only 3.53 pore volumes of CO_2 injection. Moreover, it appears that the diffusion mechanism hasten the oil recovery process thereby yielding 95.53 % incremental oil recovery in less than half of the CO_2 injection period (in 53.5 years) in the process without-diffusion. Diffusion mechanism even in immiscible process saves huge operational as well as gas compression costs especially when CO_2 is used as an injection gas. This further implies that miscibility generation may not be a prerequisite

condition for achieving the optimum oil production from the oil reservoirs through gravity drainage mechanism.

Gas-oil ratio (GOR) with-diffusion case shown a higher degree of reduction in the gas production reaching to maximum of 1.32E+05 in comparison with the maximum GOR of 5.5E+05 with no-diffusion case. Injected CO_2 diffuses through the oil phase thereby increasing the oil vaporization process resulting into the high recovery and lower GOR. Reservoir pressure behaviour during with diffusion activated is as depicted in **Figure 6-28D.** Initial phase of drop in reservoir pressure is attributed the loss of the CO_2 injectivity because of high water production in the diffusion activated simulations. Water cut as high 89% was observed during this phase which then reduced to less than 10% in the next 2 years. Reservoir pressure is dropped by 138 psi in 18 years with an annual rate of 7.77 psi per year.

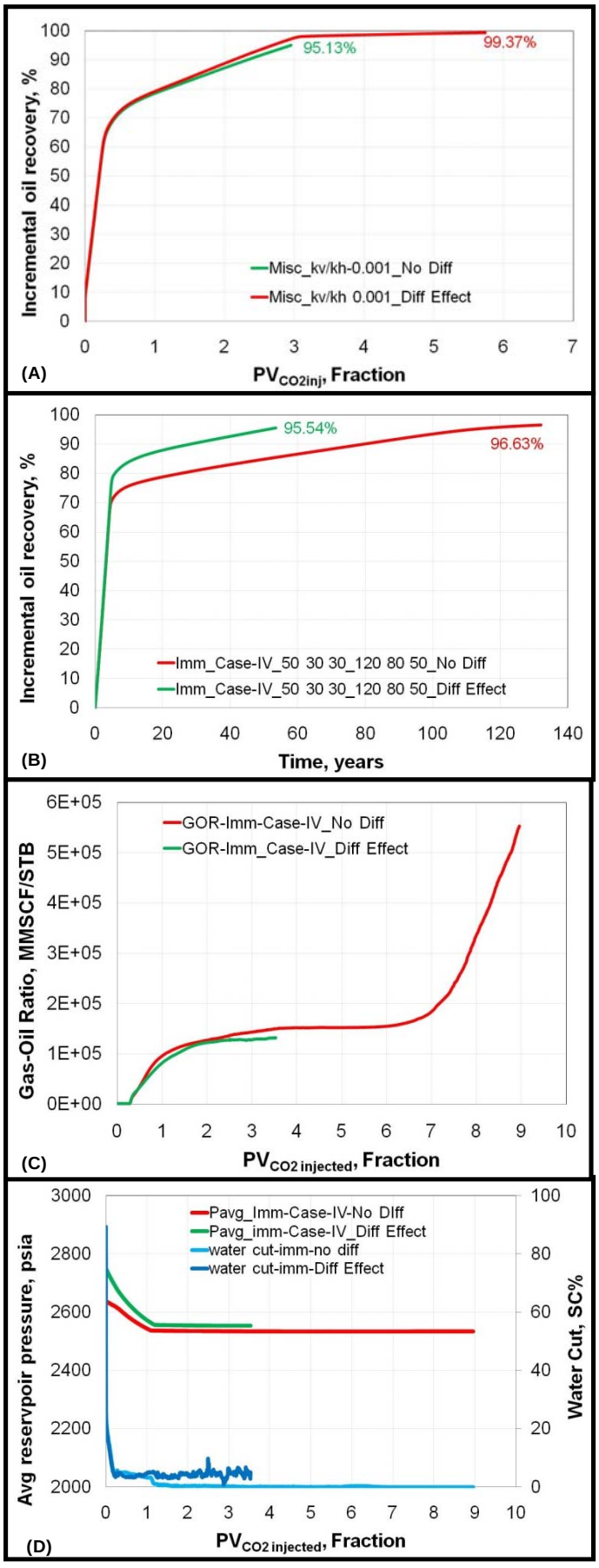

Figure 6-28: Effect of molecular diffusion in immiscible process (Case-IV, optimized grid, k_v/k_h = 1.0)

6.4.2 Heterogeneous Reservoir (k_v/k_h = 0.001)

In order to study effect of the molecular diffusion in heterogeneous reservoir, permeability in the downward direction (as oil-gravity drainage is in vertical-downward direction) is changed to 1.2 mD compared to 1200 mD in the horizontal direction.

As mentioned in the section 6.3.1, permeability heterogeneity exhibits the tendency for CO_2 to disperse in the horizontal direction through the tortuous porous media due to the higher horizontal permeability (in low k_v/k_h reservoirs) at the gas-oil interface. Results presented in **Figure 6-29** show the effect of diffusion in heterogeneous reservoir with k_v/k_h = 0.001. As mentioned in section 6.3.1, no-diffusion simulation runs yield 95.5% incremental oil recovery in only 3 pore volumes of CO_2 injection. On the other hand, diffusion case achieved even higher incremental oil than that level to 97.8% in 91 years which is 42 years earlier than the no diffusion case (**Figure 6-29A**). Moreover, it is 10% higher than the no diffusion case in the year 2063. These results again show that the active diffusion phenomenon speeds up the oil recovery process thereby saving the operational costs of the CO_2 injection and the project cost with regards to the less time taken for the optimum recovery. However, this final incremental recovery with diffusion case was only 1.5% higher than the no diffusion case especially at the same 3.16 pore volumes of CO_2 injected (PV_{CO2inj}) as depicted in **Figure 6-29B**. This result shows that the low vertical Darcy permeability (velocity) of the formation provided more residence for the concentration based cross-phase diffusion at the front and in the pores behind the floodfront. The slower downward movement of GOC because of the low oil-drainage rate, CO_2 will have more time to diffuse through the oil phase across the interface. This will be more pronounced in the horizontal direction leading to the dispersion phenomenon arising from the solute (CO_2) in the tortuous porous media. This leads to the "active diffusion phenomenon" which further enhances the efficient vaporization or extraction of the oil at the flood front, across the interface and behind the floodfront.

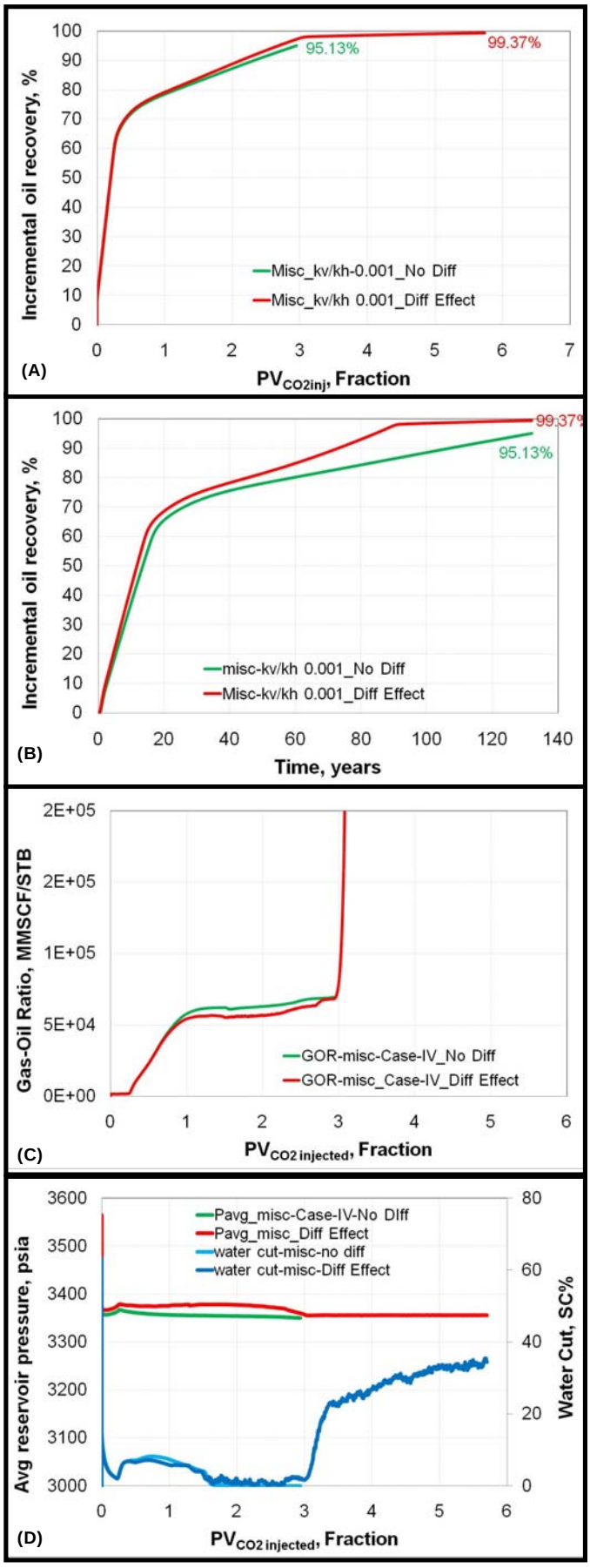

Figure 6-29: Effect of diffusion in heterogenic reservoir (k_v/k_h = 0.001; optimized grid) (Case-IV)

Figure 6-29C shows that the gas-oil ratio (GOR) in diffusion case suddenly increases vertically (2.94 PV_{CO2inj} and GOR of 68765 MMSCF/STB) at which continued to grow reaching the maximum GOR value of 1.5E+06. The corresponding pore volume of 2.94 at which this vertical rise is noticed also exhibited the incremental recovery of 97.16% (see **Figure 6-29B)**. On the other hand, no diffusion case yielded 95.06% incremental recovery which is 2% lower than the diffusion incremental recovery. Moreover, diffusion case recovery took 89 years to yield 2% higher incremental oil recovery (at same pore volume) in contrast with 132 years in no-diffusion case. This comparison shows again shows that the diffusion mechanism not only recovers the higher incremental oil but also hasten the oil recovery process. Furthermore, water production beyond 2.94 PV_{CO2inj} also starts to increase from 2% to 36% at the end. Reservoir pressure behaviour showed more stable profile (**Figure 6-29D**)

6.5 Effect of Mode of CO_2 Injection: Secondary vs. Tertiary Recovery

In studying the effects of CO_2 injection mode, tertiary mode CO_2 injection (after secondary waterflooding) is conducted in the CO_2-assisted gravity drainage EOR process through the numerical compositional simulations on the optimized grid (50 × 30 × 30: 120 ft × 80 ft × 50 ft). The results so obtained are then analysed by comparing the effects of (i) tertiary mode immiscible and miscible CO_2 injection (ii) Secondary vs. tertiary CO_2 injection in both the immiscible and miscible process.

6.5.1 Tertiary CO_2-Assisted Gravity Drainage EOR Process: Immiscible and Miscible Recovery

Literature review of the commercial gravity drainage field projects suggests that the CO_2 injection have been employed in both the secondary as well as tertiary modes, with most of them utilizing hydrocarbon gas as an injection gas in addition to nitrogen and air injection gases. Only two studies indicated the application of CO_2 as an injection: One in the Weeks Island pilot field project (32.7 ^{o}API gravity oil) yielding 60% OOIP in the tertiary immiscible flooding (Johnston, 1988). On the other hand, other field project in the Wolfcamp Reef reservoir (43.5 ^{o}API gravity oil) yield 74.8% OOIP in the tertiary miscible CO_2-flooding (Bangla et al., 1991).

In this investigation, tertiary mode CO_2 is injected in the 50 ^{o}API gravity reservoir to study its effect on the final incremental oil recovery, gas-oil ratio, water cut (%) and the

average reservoir pressure in the CO_2-assisted gravity EOR process. Diffusion effects are neglected in this study.

Figure 6-30A show that the miscible CO_2 injection yields 4% higher final incremental recovery (97%) than the incremental recovery (93%) obtained in the tertiary mode immiscible CO_2 injection. Although the immiscible incremental recovery approaches the miscible recovery towards the end, they tend to move apart from each other from the point onwards the CO_2 floodfront arrival. Tertiary miscible incremental recovery at 1, 2 and 3 CO_2 pore volumes injection (fraction) was 12%, 23% and 25% higher than their counterparts in the tertiary process. With the continued tertiary mode CO_2 injection, this difference successively reduced to only 4% in the final year January 2112 since its start in the year 1977.

These higher incremental recoveries in miscible process are attributed to the absence of the interfacial tension, so the capillary forces. On the other hand, capillary forces try to retain the oil in pores (capillary retention) causing lower incremental oil recoveries. Moreover, water-shielding of the oil trapped in pores further makes this inaccessible. However, the interfacial tension differences between the water, water and gas under gravity drainage condition causes this retained left-behind oil in the pores to connect to form oil blobs and then a 'thin oil film' (Chatzis et al., 1988; Kalaydjian, 1992). This flows between water and injected CO_2 and drains the oil behind floodfront downward towards the production wells, leading to very low residual oil saturation. Linearly increasing incremental oil recovery in tertiary immiscible process (**Figure 6-30A**) is caused by this slow "oil-film flow" phenomenon.

Gas-oil ratio (GOR) in the miscible process was 41000 and 80000 MMSCF/STB respectively at the 1 and 2 pore volumes of CO_2 injection respectively. It exhibited near-vertical sharp rise to reach 2.8E+05 MMSCF/STB in only 8 years of 1 PV_{CO2} injection. On the other hand, GOR in the immiscible process shown sharp rise up to 90000 MMSCF/STB in the 1 pore volumes of CO_2 injection (fraction), which is then arrested to exhibit the near-horizontal flat profile to reach 1.25E+05 MMSCF/STB. It gradually kept rising to gain only 35000 MMCF/STB in the next 80 years (1997 to 2077) to reach 1.60E+05 MMSCF/STB.

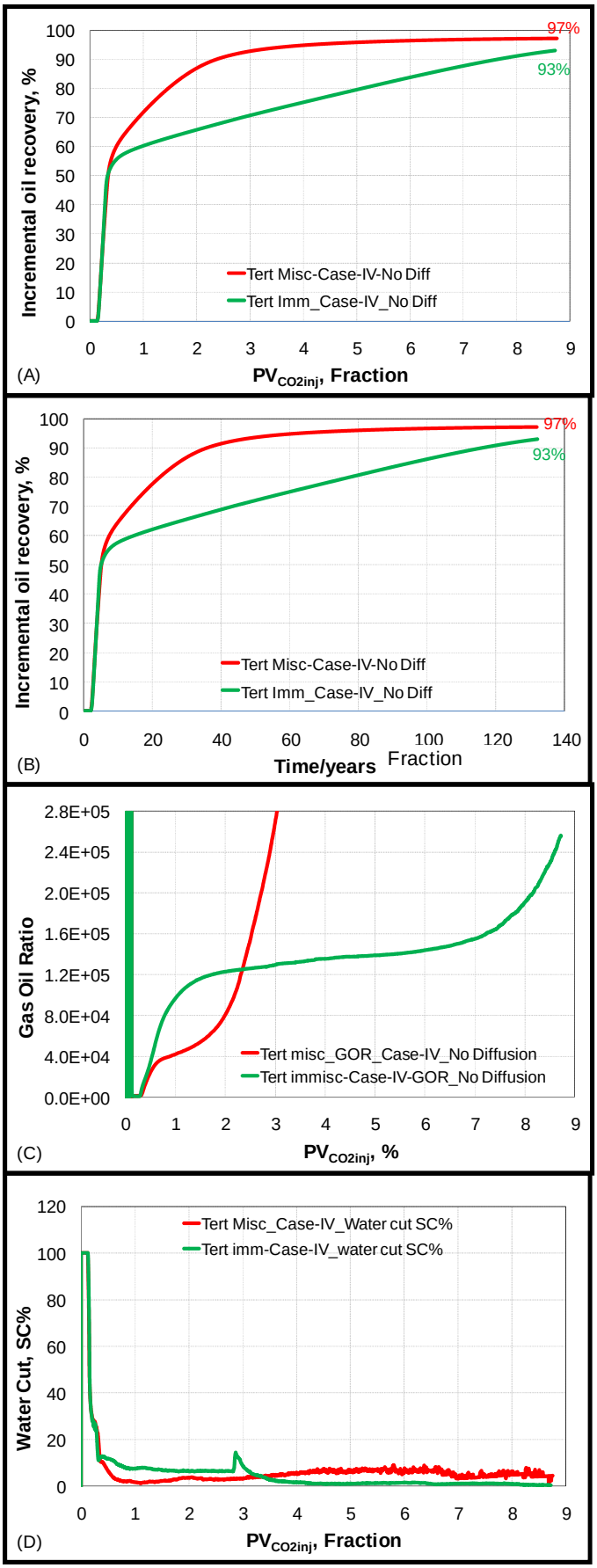

Figure 6-30: Immiscible vs. miscible process performance in the *tertiary* CO_2-assisted gravity drainage EOR process (optimized grid: 50 × 30 × 30: 120 ft × 80 ft × 50 ft; k_v/k_h = 1.0)

Corresponding water production profile shown in **Figure 6-30D** demonstrates that the water continue to produce completely until oil phase reached the horizontal production wells 1.9 years later in February 1979. It then dropped less than 10% for the remaining tertiary CO_2 immiscible and miscible CO_2 injection.

Figure 6-31 shows that the average reservoir pressure drop is very low in the tertiary CO_2-assisted gravity drainage EOR process since the arrival of oil phase in the horizontal production wells in February 1979 in spite of the increasing GOR. It dropped by 38.86 psia (2623 psia to 2585 psia) and 28.75 psia (3590.79 psia to 3562 psia) in the immiscible and miscible process respectively at the end in January 2109. It means that the annual drop in the reservoir pressure was 0.22 and 0.3 psia in the immiscible and miscible process respectively over 126 years. This average reservoir pressure behaviour in turn is indicates that the respective pressure in the gas-cap would be constant, thereby satisfying Cardwell and Parsons (Cardwell and Parsons, 1949b) criteria of free gravity drainage.

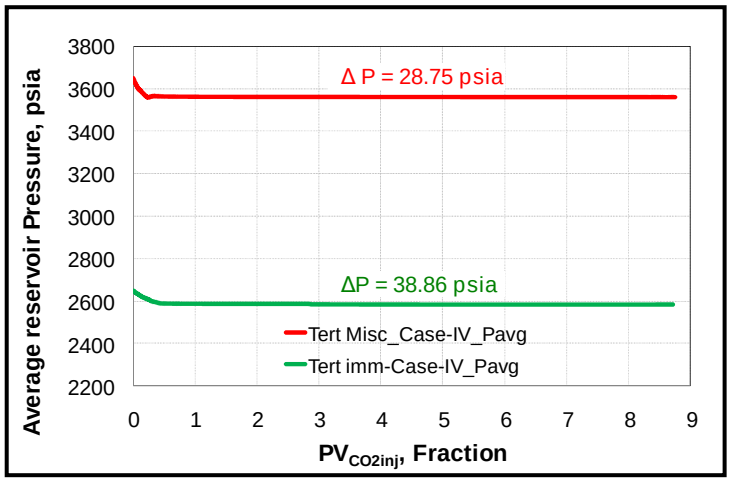

Figure 6-31: Average reservoir pressure profile during *tertiary* mode immiscible and miscible CO_2-assisted gravity drainage EOR process (optimized grid: 50 × 30 × 30: 120 ft × 80 ft × 50 ft; k_v/k_h = 1.0)

Effect of the tertiary mode immiscible and miscible CO_2 injection in CO_2-assisted gravity drainage EOR process is represented in **Figure 6-32 (A through D)** through the oil viscosity, gas saturation and oil saturation changes occurring in block (25, 14, 23). **Figure 6-32A** shows that the oil viscosity in this representative block increased from 0.16 cP (15 February 1979) to 0.24 cP (in January 2082) in 103 years. Gas saturation showed very gradual increase while the respective oil in this block continues to drain gradually (**Figure 6-32B)**. This further suggests that the oil continued to drain slowly through film. Literature review suggested that the CO_2 vaporizes the reservoir even in immiscible mode (Mungan,

1982). Oil viscosity increase profile along with the gradual gas saturation rise further confirms this gradual oil vaporization by CO_2 simultaneously with the oil film flow. Residual oil saturation in this block was 0.08.

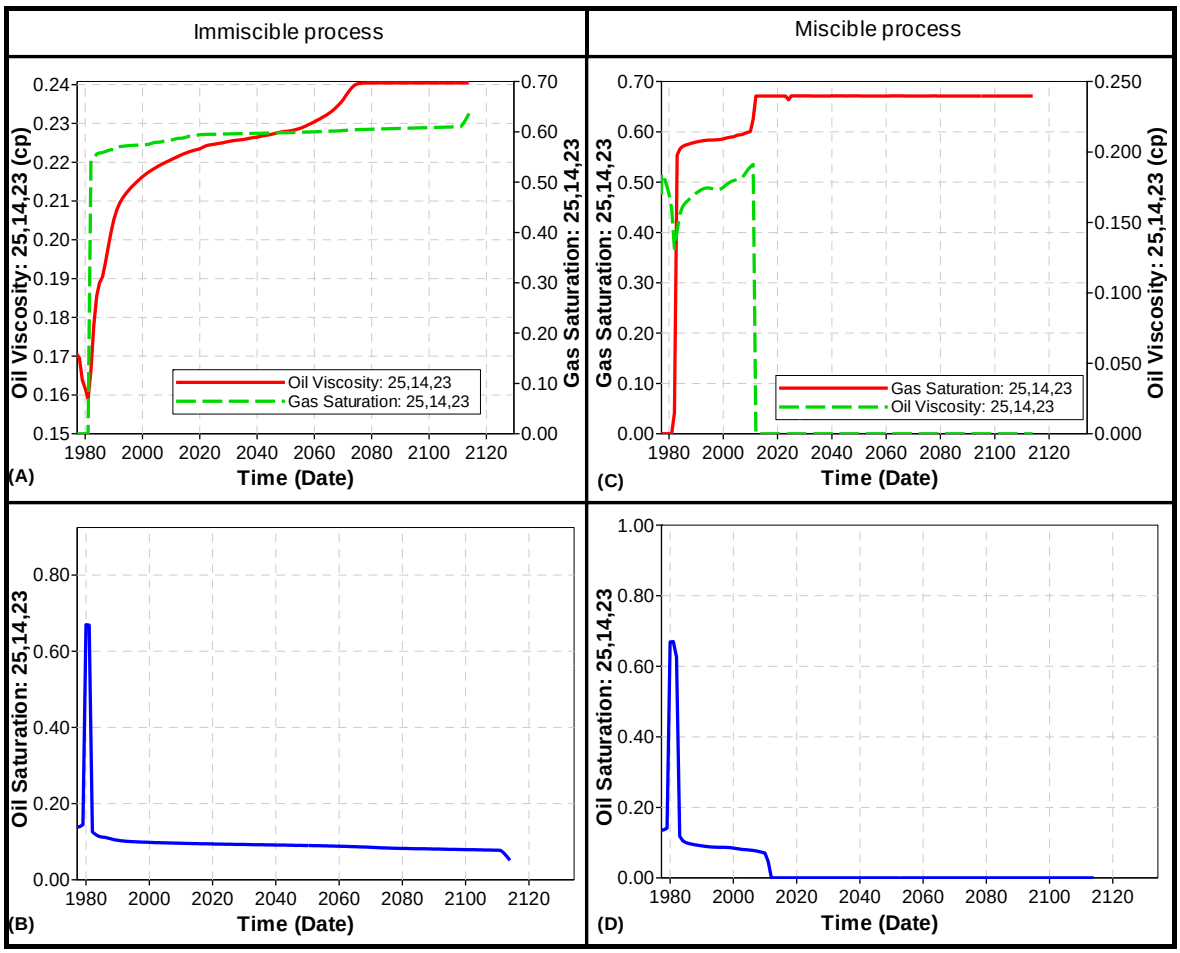

Figure 6-32: Oil viscosity, gas and oil saturation profile during *tertiary* mode immiscible/miscible CO_2-assisted gravity drainage EOR process (optimized grid: 50 × 30 × 30: 120 ft × 80 ft × 50 ft; k_v/k_h = 1.0)

In miscible process, the oil viscosity increases, as shown **Figure 6-32C,** from 0.14 in February 1979 to 0.2 in January 2022 after initial oil swelling. Corresponding gas saturation increased in accordance with the oil viscosity suggesting that the CO2 did vaporization the oil during the ongoing gradual oil production. The respective oil saturation eventually reduced to zero with the continued vaporization of medium as well as heavy fractions of oil leading to the complete recovery from this block (**Figure 6-32D**). Miscible process yield complete recovery (end S_o = 0.0) from block (25, 14, 23) in less than half years of CO_2 flooding (46 years) compared to 0.08 oil saturation in the immiscible flooding.

Results presented in **Figure 6-30B**, **Figure 6-32A** through **Figure 6-32D** further indicates that the oil vaporization mechanism by CO_2 in miscible process is capable of yielding faster recovery (less years) than the oil film flow and the oil vaporization mechanism in the immiscible process.

Moreover, the 'diffusion mechanism' further enhances and hastens incremental recovery in the tertiary miscible CO_2-assisted gravity drainage process. It recovered 94.78% incremental oil in only one-third of the PV_{CO2inj} (2.6 pore volumes) (**Figure 6-33A)** and the oil production time (36 years) (**Figure 6-33B)** compared to the miscible process in the absence of diffusion mechanism. On the other hand, numerical simulations with diffusion option activated in the tertiary immiscible process produced the same incremental oil (93%) in 7.6 PV_{CO2inj} (**Figure 6-33A)** and 12 years less (**Figure 6-33B)** than their immiscible counterparts without diffusion option. These results further indicate that the diffusion mechanism is active in both the miscible and immiscible CO_2-assisted gravity drainage EOR process. Keeping in mind the operational and CO_2 compression costs during the life of an EOR project, tertiary miscible CO_2-assisted gravity drainage EOR process looks to be a viable recovery process.

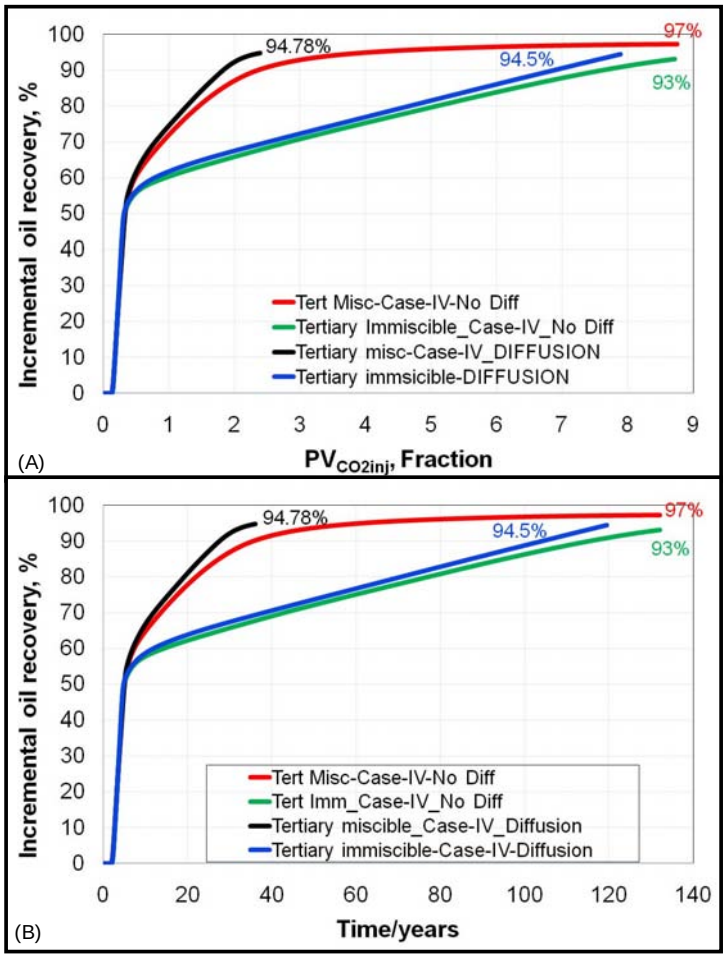

Figure 6-33: Effect of diffusion phenomenon on the incremental EOR in the *tertiary* mode immiscible and miscible CO_2-assisted gravity drainage EOR process

6.5.2 Secondary vs. Tertiary CO_2-Assisted Gravity Drainage EOR Process Comparison

Commercial gravity drainage EOR projects have been employed in both the secondary and tertiary modes of CO_2 injection (see section 2.3.6) in the CO_2-assisted gravity drainage EOR method. Literature review carried out in this study suggested that none of the reported investigations/field projects used CO_2 as an injection gas in the secondary mode injection. Both the two reported cases used tertiary mode CO_2 injection in that achieved maximum oil recovery of 74.8% OOIP.

To study effect of the injection mode, results of the tertiary mode CO_2-assisted gravity drainage process (previous section 6.5.1) are compared with the results from secondary mode CO_2-assisted gravity drainage process (previous section 6.5.1). Recovery performance in both the immiscible and miscible process is analysed using the final

incremental oil recovery, gas-oil ratio, water cut and the average reservoir pressure over the entire CO_2 flooding operation.

6.5.2.1 Immiscible process performance

Immiscible process performance is shown in **Figure 6-34A** through **Figure 6-34D** demonstrate that the mode of gas injection significantly affect the oil recovery performance of the CO_2-assisted gravity drainage EOR process. Tertiary mode incremental recoveries are significantly lower than those in secondary mode recoveries. At 0.3 Pore volumes of CO_2 injection (PV_{CO2inj}) the tertiary process yield 48% incremental recoveries, which is 20% lower than the secondary process recoveries (68%). Beyond this gas breakthrough stage, both the modes of CO_2 injection continued to recover the incremental oil linearly for 132 years. At 3 PV_{CO2inj}, difference of the incremental recovery was 14%. Tertiary final incremental recovery was 93.2%, about 4% lower than 97.03% recovery in secondary process after 8.7 and 9 PV_{CO2inj}. This result indicates that secondary immiscible process clearly outperforms the tertiary immiscible CO_2-assisted gravity drainage EOR process.

In secondary process, oil production immediately starts without delay in breakthrough at production wells. This is reflected in the higher GOR in secondary immiscible CO_2 injection than the tertiary immiscible process (See **Figure 6-34C)** although the secondary recovery was achieved at the producing GOR equal to solution GOR until gas breakthrough. On the other hand, oil phase took 1.9 years in tertiary process to reach horizontal wells production wells once water from the waterflooded-oil zone is swept away by the approaching oil phase. This is clearly seen in **Figure 6-34D** that 100% water production is observed during this phase. Water constitutes the majority of the production before gas breakthrough. Moreover, mobile water during tertiary phase gas injection incurs three phase production at the producing wells. Water production during tertiary EOR process was higher (waterflooded-oil zone retain some of the water even after its sweeping by tertiary mode CO_2 assisted oil-phase displacement) than the water production during secondary mode CO_2-assisted gravity drainage EOR process.

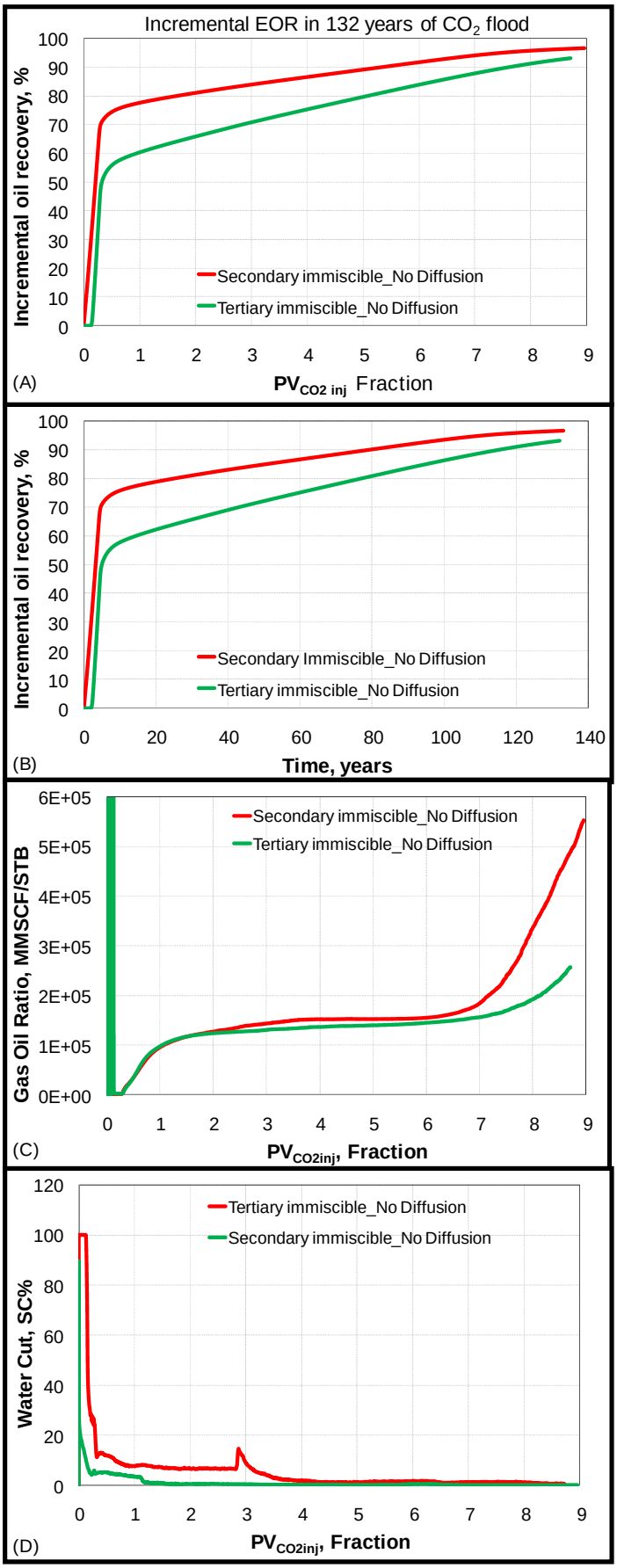

Figure 6-34: Secondary vs. Tertiary *immiscible* CO_2-assisted gravity drainage EOR process performance comparison (optimized grid: 50 × 30 × 30: 120 ft × 80 ft × 50 ft; k_v/k_h = 1.0)

Average reservoir pressure profile in both the tertiary and secondary immiscible CO_2-assisted gravity drainage EOR process is as shown in **Figure 6-35A** and **Figure 6-35B.** In tertiary immiscible process it dropped from 2650 psi to 2585 psi in 126 years with the average annual pressure drop of 0.5 psi/year. Moreover, it dropped by 12.14 psi/year from 2650 psi (11 March 1977) to 2589 psi (February 1984) 7 years which then stabilized to drop to 2585 in 119 years. On the other hand, secondary immiscible process experienced the average reservoir pressure drop of 105 psi in 132 year with an annual rate of 0.8 psi/year. Moreover, it dropped from 2638 psi (6 January 1972) to 2538 psi (28 August 1988) leading to annual drop-rate of 6 psi/year. Average reservoir pressure then reduced by only 4 psi in the remaining years of production until January 2105.

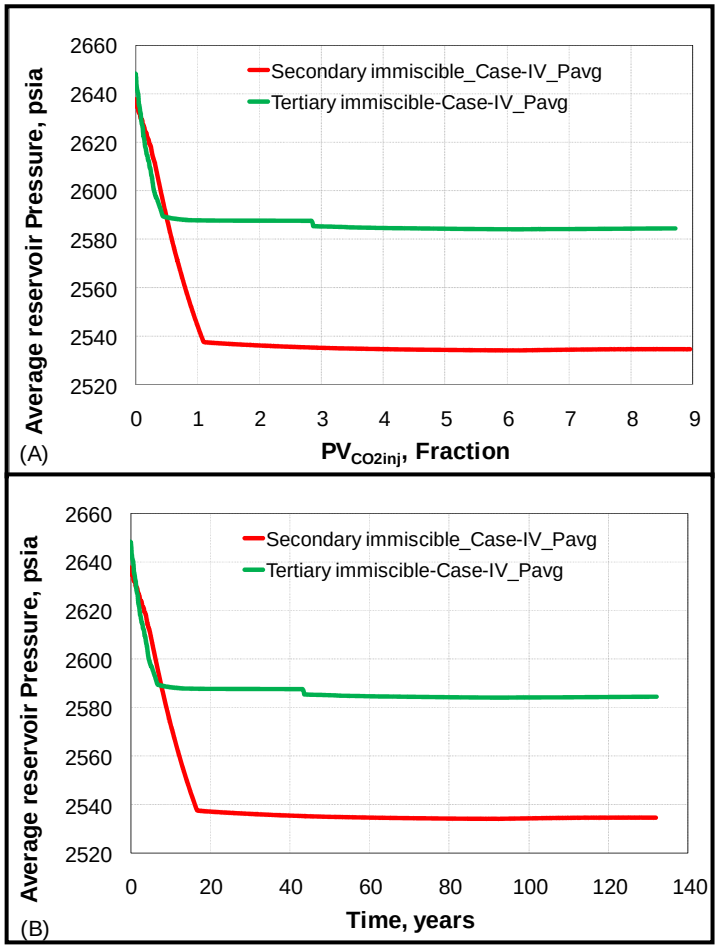

Figure 6-35: Effect of Secondary vs. Tertiary mode CO_2 injection on *immiscible* CO_2-assisted gravity drainage EOR process (optimized grid: 50 × 30 × 30: 120 ft × 80 ft × 50 ft; k_v/k_h = 1.0)

6.5.2.2 Miscible process performance

Incremental oil recovery performance depicted in **Figure 6-36A** shows that secondary and tertiary mode of CO_2 injection do not show significant effect in CO_2-assited gravity drainage EOR process. Incremental recoveries at gas breakthrough (at the time when gas floodfront arrived), 1, 2 and 3 PV_{CO2inj} are 50%, 72%, 88% and 93% in tertiary process in comparison with the 68%, 83%, 91% and 94.46% in the secondary process respectively. Further comparative analysis shows that the tertiary mode incremental recoveries closely approach the secondary mode incremental recoveries successively from 18% at gas breakthrough to 11%, 3% and 1.5% respectively. In another 1 PV_{CO2inj}, this difference of incremental recoveries approaches to 1% which remained same for the entire 132 years of CO_2 injection in both the secondary and tertiary mode. Final incremental recovery in secondary and tertiary CO_2 miscible flood was 98.34% (8.92 PV_{CO2inj}) and 97.25% (8.75 PV_{CO2inj}) respectively. These results further signify that the mode of CO_2 injection does not have significant impact on the final incremental oil recovery in the miscible CO_2-assisted gravity drainage EOR process.

Moreover, GOR in both the secondary and tertiary miscible flood remained close to each other's level at which 94.46% and 93% incremental oil was recovered respectively (**Figure 6-36C**). Beyond this production phase, GOR in tertiary CO_2 miscible flood starts to exhibit higher trend than the secondary miscible flood. In secondary process, oil production immediately starts without delay in breakthrough at production wells. On the other hand, oil phase took 1.9 years in tertiary process to reach horizontal wells production wells once water from the waterflooded-oil zone is swept away by the approaching oil phase. This is clearly seen in **Figure 6-36D** that 100% water production is observed during this phase. Moreover water production during tertiary EOR process was higher (waterflooded-oil zone retain some of the water even after its sweeping by tertiary mode CO_2 assisted oil-phase displacement) than the water production during secondary mode CO_2-assisted gravity drainage EOR process.

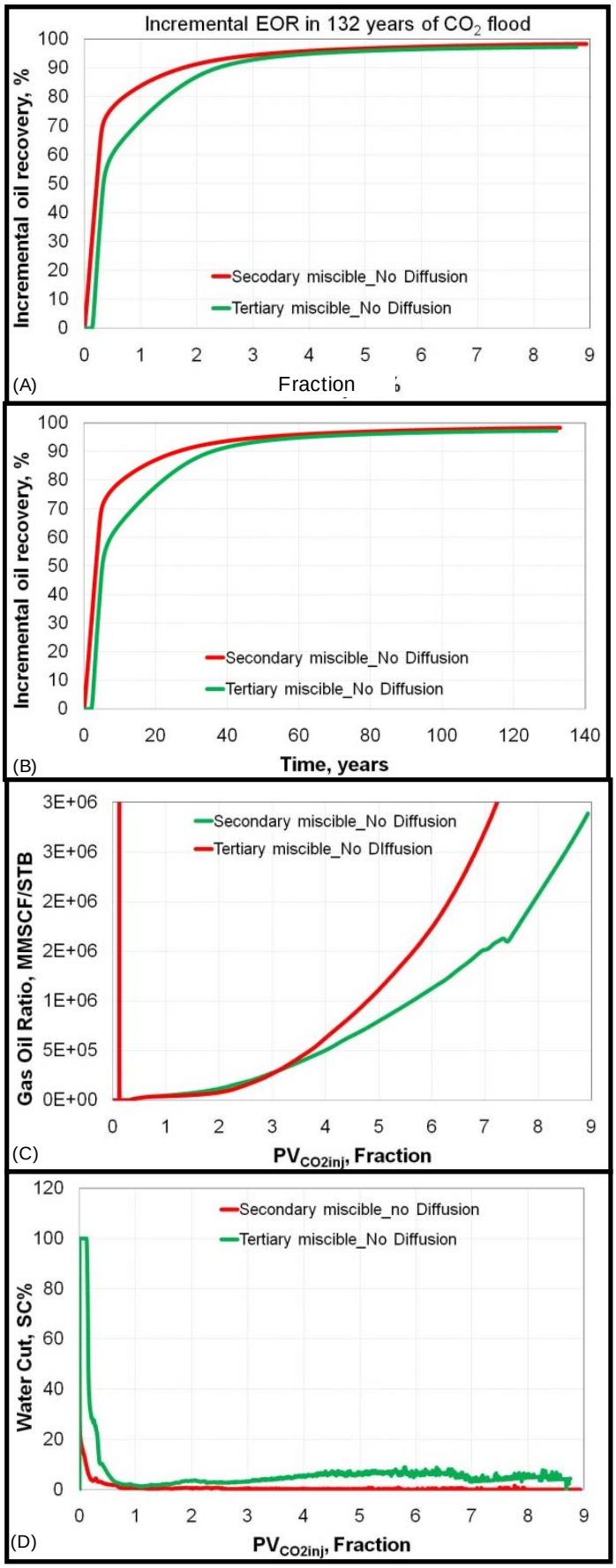

Figure 6-36: Effect of the secondary vs. tertiary mode of CO_2 injection in the *miscible* CO_2-assisted gravity drainage EOR process (optimized grid: 50 × 30 × 30: 120 ft × 80 ft × 50 ft; k_v/k_h = 1.0)

Average reservoir pressure profile in both the tertiary and secondary miscible CO_2-assisted gravity drainage EOR process is as shown in **Figure 6-37A** and **Figure 6-37B.** In tertiary miscible process it dropped from 3650 psi to 3561 psi in 126 years with the average annual pressure drop of 0.71 psi/year. Moreover, it dropped by 25 psi/year from 3650 psi (4 April 1977) to 3560 psi (January 1984) in 3.5 years which then stabilized to 3561 psi in 119 years. On the other hand, secondary miscible process experienced the average reservoir pressure drop of 182 psi in 132 year with an annual rate of 1.2 psi/year. Moreover, it dropped from 3680 psi (2 February 1972) to 3518 psi (12 November 1981) leading to annual drop-rate of 16 psi/year. Average reservoir pressure then reduced by only 4 psi in the remaining years of production until 1 January 2105.

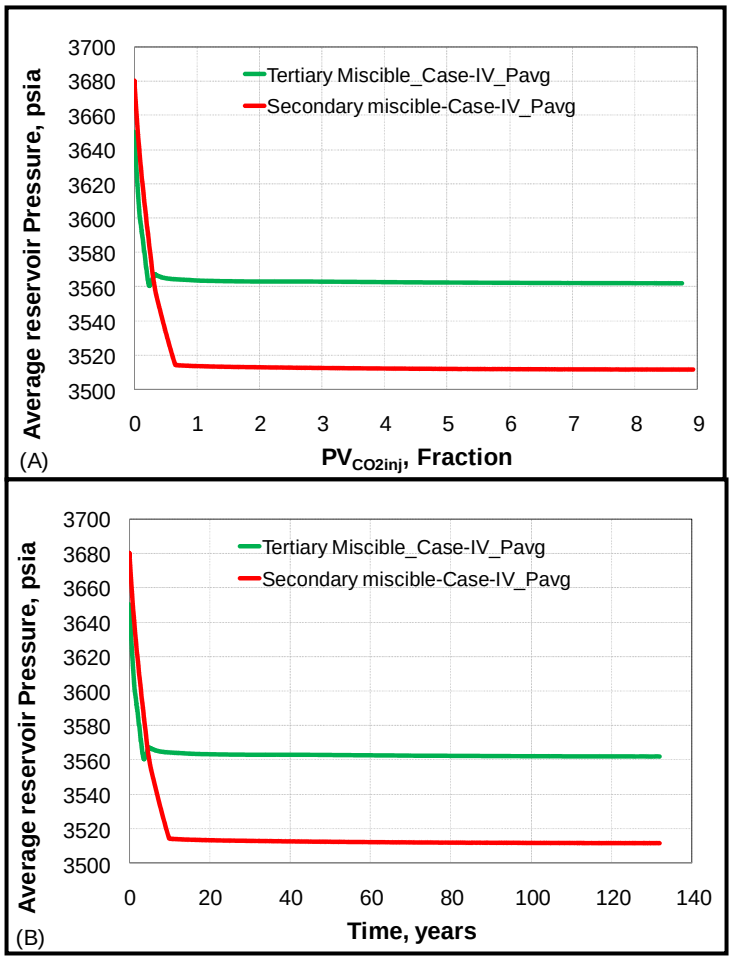

Figure 6-37: Effect of secondary vs. tertiary mode of CO_2 injection on average reservoir pressure in miscible CO_2-assisted gravity drainage EOR process

6.5.2.3 Comparative analysis

In order to assess the effectiveness of mode of gas injection on the incremental oil recovery, the comparative average oil saturation at the end of CO_2 flooding is as depicted in **Figure 6-38A** and **Figure 6-38B.** This comparison, in addition to results presented in section **Figure 6-34A** and **Figure 6-34B; Figure 6-36A** and **Figure 6-36B,** clearly demonstrates that the secondary mode of CO_2 injection outperform the tertiary mode of CO_2 injection in the CO_2-assisted gravity drainage EOR process. Lower average saturation of oil phase is obtained in secondary process than the ones obtained in the tertiary process.

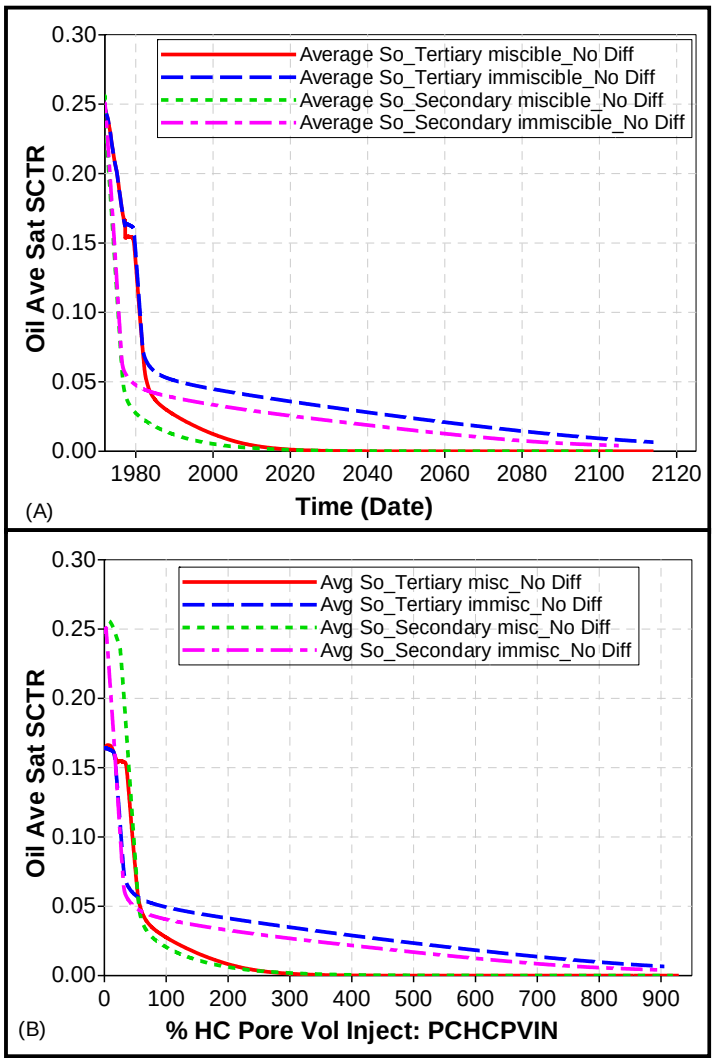

Figure 6-38: Comparison of average oil saturation at the end of secondary and tertiary mode CO_2 injection in both the immiscible and miscible CO_2-assisted gravity drainage EOR process (optimized grid: 50 × 30 × 30: 120 ft × 80 ft × 50 ft; k_v/k_h = 1.0)

Secondary mode immiscible CO_2 injection resulted in lower average residual oil saturations (0.0044) than the tertiary immiscible CO_2 injection mode (0.0066) at the end of

the recovery process in January 2105. It needed close to 8.75 pore volumes of CO_2 injection over 132 years.

6.6 Voidage Replacement during CO_2-Assisted Gravity Drainage Oil Recovery

During gas flooding operations, especially the ones that proceed under the gravity drainage mechanism, the balance of the volume of gas injected and the simultaneous withdrawal of the total reservoir fluids (oil, solution and free gas, and the water) plays an important role in keeping oil recovery in the gravity drainage regime. If the total volume of fluid production from the producing formation is more than the volume of gas injected, the reservoir voidage is created, that tend to decrease the reservoir pressure. In other words the voidage replacement ratio (VRR), which is the ratio of the volume of the gas injected to the volume of the total fluids produced, is less than the 1.0. Conversely, the higher gas injection volume with relative to the total fluid withdrawal volume, the reservoir pressure keeps rising (VRR greater than 1.0). This implies that the oil recovery may or may not come from the gravity drainage mechanism. It solely depends upon the rate at which the gas is being injected. It is assumed during these considerations that there is no out-of-zone injection loss from the target zone or severe thieving or influx of fluids occurring.

$$\text{Voidage Replacement Ratio (VRR)} = \frac{\text{Volume of gas injected } (V_{inj})}{\text{Volume of fluid produced } (V_{prod})}$$

For gas flooding operations,

$$VRR = \frac{i_g.B_g}{Q_oB_o + Q_wB_w + (Q_g - R_sQ_o)B_g}$$

On the other hand, the gas injection volumes higher than that of the total fluid withdrawal volumes indicate that the viscous forces could be dominating the oil recovery. Moreover, the viscous forces arising from the rate of the gas injection are needed to be balanced against the opposing buoyancy forces. This puts limit to the rate of the gas injection, so the volume of the gas injected. Beyond this gas injection rate, the oil recovery no longer comes from the gravity drainage mechanism; rather it would be the viscous

dominated one. This needs to be addressed while considering the voidage replacement aspects of the gravity drainage gas flooding operations.

6.6.1 New concepts: Critical (i_{gc}) and stable (i_{gs}) Gas Injection Rates; Critical Voidage Replacement Ratio (VRR_C)

As mentioned in the previous section, the maximum velocity, (so the gas injection rate, i_g), at which gas will not finger through the oil phase, thus its premature breakthrough in the producing wells, is termed as critical velocity, u_c. Beyond this velocity, the oil recovery mechanism shifts from the gravity dominated to the viscous dominated regime. This concept can be introduced in terms of the voidage replacement ratio (VRR). The maximum gas injection rate at which the gas fingers through is termed as the critical rate of the gas injection, i_{gc}. By introducing i_g in the form of the volumetric gas injection for the given specified time, voidage replacement ratio can be defined as the ratio of the maximum allowable volume of the gas injection to the respective total fluid volume produced.

$$VRR_c = \frac{\text{maximum allowable critical volume of the gas injected}}{\text{Volume of the reservoir fluid produced}}$$

$$VRR_c = \frac{V_{gc}}{V_{prod}}$$

According to the criteria hypothesized by Dumore (1964) for the miscible gas flooding, the critical velocity of gas injection is

$$u_c = \frac{i_g}{A} = \left(\frac{\rho_o - \rho_s}{\mu_o - \mu_s}\right) kg$$

$$\text{Critical rate (Volumetric) of gas injection, } i_{gc} = u_c \times A = \left(\frac{\rho_o - \rho_s}{\mu_o - \mu_s}\right) kg \times A$$

$$\text{Critical volume of the gas injection, } V_c = u_c \times A \times \text{time} = \left(\frac{\rho_o - \rho_s}{\mu_o - \mu_s}\right) kg \times A \times \text{time}$$

$$\therefore VRR_c = \frac{i_{gc} \times \text{time}}{V_{prod}} = \frac{\left[\left(\frac{\rho_o - \rho_s}{\mu_o - \mu_s}\right) kg \times A \times \text{time}\right].B_g}{V_{prod}}$$

Similarly the VRR for the stable gas injection rate can be the given by the equation

$$\therefore VRR_{st} = \frac{i_{gst} \times time}{V_{prod}} = \frac{\left(\frac{\rho_o - \rho_s}{\mu_o - \mu_s}\right) kg \times A \times time}{V_{prod}}$$

6.7 Summary

Results of the reservoir simulations on the base model identified the operational mechanisms immiscible and miscible CO_2-assisted gravity drainage EOR process. Comparative evaluation of the incremental oil recoveries at seven injection and production well rate-constraint combinations resulted in the development of a general process selection map. Grid dimensions and thickness studies lead to the use of the optimized model in the next phase of the simulation runs. Comparative evaluation of the oil recovery performance in the CO_2-assisted gravity drainage EOR process is conducted to study the effects of the miscibility generation, mode of gas injection, heterogeneity in permeability and porosity and the molecular diffusion. Investigation of the relative effectiveness of the immiscible and miscible process compounding mechanisms provided the guidelines to draw important conclusions in this study. Interacting multiphase operational parameters were identified from the reservoir simulation study and are applied in the scaling and sensitivity analysis of the CO_2-assisted gravity drainage EOR process through the development of the scaled models in the next Chapter.